ELUCIDATION OF POSSIBLE IRON REDUCTION MECHANISMS IN KAOLIN BIOLEACHING BY *BACILLUS* SPECIES

YONG SHIH NEE

MASTER OF SCIENCE

LEE KONG CHIAN FACULTY OF ENGINEERING AND SCIENCE
UNIVERSITI TUNKU ABDUL RAHMAN
MAY 2022

ELUCIDATION OF POSSIBLE IRON REDUCTION MECHANISMS IN KAOLIN BIOLEACHING BY *BACILLUS* SPECIES

By

YONG SHIH NEE

A dissertation submitted to the Department of Mechanical and Material Engineering,
Lee Kong Chian Faculty of Engineering and Science,
Universiti Tunku Abdul Rahman,
in partial fulfillment of the requirements for the degree of
Master of Science
May 2022

ABSTRACT

ELUCIDATION OF POSSIBLE IRON REDUCTION MECHANISMS IN KAOLIN BIOLEACHING BY *BACILLUS* SPECIES

Yong Shih Nee

Kaolin minerals contain Fe impurities which affects its commercial value and refractory properties. Chemical treatments and physical techniques are able to remove these impurities but are associated with high environmental impact and cost. To circumvent these negative impacts, recent efforts have been focused on the use of bioleaching where kaolin is treated with microorganisms. Early results established a noticeable effect of the bacteria on the redox state of structural Fe, but knowledge gaps persist in terms of details on the bacterial-kaolin interactions such as electrostatic charges and bond formation during attachment of bacteria onto mineral surface. Moreover, information on the metabolites produced by bacteria and its effects on Fe(II)/Fe(III) ion equilibria in solution remains scarce. Hence, the ability and mechanisms of *Bacillus* sp. in Fe(III) reduction in kaolin bioleaching was studied. In this work, 20 g of kaolin powder with 9×10^8 CFU of *Bacillus cereus, Bacillus aryabhattai* and *Bacillus megaterium* were incubated in 200 mL of 10 g/L glucose medium respectively for 10 days at 30°C with 250 rpm. Based on phenanthroline results, all samples treated with bacteria showed increasing trends in Fe(III) reduction up until day 6 or 8 followed by a slight decrease towards the end of the ten-day period. For kaolin treated with *B. cereus*, the Fe(II) concentration increased gradually and had the highest extent

of Fe(III) reduction at day 8, which is 1.43 µg/mL of Fe(II) in solution. Both of the kaolin treated with *B. aryabhattai* and *B. megaterium* reached a maximum of Fe(II) concentration at day 6, which were 1.26 µg/mL and 1.25 µg/mL respectively. Besides, EDS results showed the removal of Fe did not cause significant changes on chemical composition of other elements. Glucose concentration in the medium was shown to decrease progressively during bioleaching, an indication of glucose consumption by bacteria for cellular respiration. During the cell growth, *B. cereus* produced malate and acetate. For *B. aryabhattai*, malate, acetate, succinate, formate and lactate were detected whereas malate, acetate and lactate were produced by *B. megaterium*. The presence of organic acids was also confirmed by a decrease of pH values in the medium at the end of the bioleaching period. While the organic acids produced were responsible in reducing Fe(III) to Fe(II), SEM images showed bacterial activities damaged the edges of kaolin particles which appears to be sharper. However, XRD indicated that there was no formation of secondary mineral phases and no structural modification in kaolin was observed after bioleaching. In bacterial-kaolin interaction, FTIR test suggested that *Bacillus* sp. attached on the kaolin surfaces through the positive site of Fe(III) with OH (of the polysaccharides parts) of the EPS. The interaction of bacterial cells with kaolin surface altered the charge values of the solution which varies with pH value and bioleaching duration, confirmed by zeta potential measurements. In short, *Bacillus* sp. is shown to be able to reduce Fe(III) efficiently from kaolin. Although previous studies indicated the presence of organic acids during the bacterial growth, the concentrations of those acids have not been measured. Studies to date also did not specify mechanism of attachment of bacterial cell on

kaolin surface in relation to production of acids and surface properties. In this study, a model involves attachment of bacterial cell on kaolin surface where positive Fe(III) site binds with OH (polysaccharide portion) of EPS through hydrogen bonding as well as production of organic acids by bacterial cell to reduce Fe(III) in kaolin to soluble Fe(II) in kaolin bioleaching by *Bacillus* species was proposed based on the surface, structural and chemical results obtained.

ACKNOWLEDGEMENT

First of all, I would like to express my sincere gratitude to my supervisor, Dr. Kuan Seng How for his patience, motivation and continuous support in helping me to complete my master research. My completion of this research could not have been accomplished without the guidance of him. My sincere thanks also goes to my co-supervisors, Dr. Steven Lim and Dr. Sylvia Chieng for always sharing their immense knowledge to overcome the challenges uncounted throughout this research.

I am grateful for the lab assistants from UTAR and UKM for teaching and guiding me to operate the instrumentation that required in this research. Besides, I would like to thank my fellow labmates in Molecular Biology Lab 5B, UKM who are Dr. Yip Chee Hoo, How Shu Sian, Sam Janeeca, Asqwin and Muhammad. They always provide me insightful suggestions and assistance which is useful in troubleshooting the results. In addition, special thanks to my labmates in UTAR, Chai Yi Jun and Wee Wei Qing for the stimulating discussions and their generosity in sharing their knowledge.

Furthermore, deepest gratitude to my caring family and friends. Their encouragement and moral support during the difficulty are much appreciated. It was a great comfort and relief to know that they are always by my side all the time. Last but not least, this work was supported by Universiti Tunku Abdul Rahman (UTAR) through UTAR Research Fund (UTARRF) under project number IPSR/RMC/UTARRF/2019-C2/K04.

APPROVAL SHEET

This dissertation entitled "**ELUCIDATION OF POSSIBLE IRON REDUCTION MECHANISMS IN KAOLIN BIOLEACHING BY *BACILLUS* SPECIES**" was prepared by YONG SHIH NEE and submitted as partial fulfillment of the requirements for the degree of Master of Science at Universiti Tunku Abdul Rahman.

Approved by:

_____
(Dr. KUAN SENG HOW)   Date: 31.5.2022
Assistant Professor/Supervisor
Department of Mechanical and Material Engineering
Lee Kong Chian Faculty of Engineering and Science
Universiti Tunku Abdul Rahman

_____
(Dr. STEVEN LIM)   Date: 31.5.2022
Assistant Professor/Co-supervisor
Department of Chemical Engineering
Lee Kong Chian Faculty of Engineering and Science
Universiti Tunku Abdul Rahman

_____
(Dr. SYLVIA CHIENG)   Date: 31.5.2022
Assistant Professor/Co-supervisor
Department of Biological Sciences and Biotechnology
Faculty of Science and Technology
Universiti Kebangsaan Malaysia

LEE KONG CHIAN FACULTY OF ENGINEERING AND SCIENCE

UNIVERSITI TUNKU ABDUL RAHMAN

Date: 31 May 2022

SUBMISSION OF DISSERTATION

It is hereby certified that **Yong Shih Nee (20UEM00898)** has completed this dissertation entitled "ELUCIDATION OF POSSIBLE IRON REDUCTION MECHANISMS IN KAOLIN BIOLEACHING BY *BACILLUS* SPECIES" under the supervision of Dr. Kuan Seng How from the Department of Mechanical and Material Engineering, Lee Kong Chian Faculty of Engineering and Science, Dr. Steven Lim from the Department of Chemical Engineering, Lee Kong Chian Faculty of Engineering and Science, and Dr. Sylvia Chieng from Department of Biological Sciences and Biotechnology, Faculty of Science and Technology (UKM).

I understand that the University will upload softcopy of my dissertation in pdf format into UTAR Institutional Repository, which may be made accessible to UTAR community and public.

Yours truly,

_____
(Yong Shih Nee)

DECLARATION

I hereby declare that the dissertation is based on my original work except for quotations and citations which have been duly acknowledged. I also declare that it has not been previously or concurrently submitted for any other degree at UTAR or other institutions.

YONG SHIH NEE

Date: 31 May 2022

TABLE OF CONTENTS

LIST OF TABLES

LIST OF FIGURES

CHAPTER 1

INTRODUCTION

1.1 Introduction

Kaolin is one of the raw materials found in clay which is rich in kaolinite ($Al_2Si_2O_5(OH)_4$) (Uddin, 2018). It is a raw material important for great variety of industrial applications, such as production of white ceramic and cement as well as manufacture of paper (Moraes et al., 2017). However, iron on the raw kaolin surface will undergo atmospheric rusting in the presence of water and oxygen to form Fe(III) oxides or oxyhydroxides which is known as rust (Thirumalai, 2020). This reddish-brown compound will affect the quality of kaolin due to its insufficient whiteness (Zegeye et al., 2013). Therefore, the iron impurities from kaolin have to be reduced to meet commercial specifications.

Conventional chemical and physical treatments such as froth flotation, gravity separation, magnetic separation, reductive heating and acid treatment (Guo et al., 2010) are able to extract iron from kaolin minerals. However, these treatments come with considerable disadvantages such as environmental pollution, high operating costs, and high energy requirements (Hosseini and Ahmadi, 2015). Hence, conventional methods are increasingly being replaced by bioleaching method for iron removal from kaolin minerals.

Bioleaching is a process of extracting metals from low-grade ores which involves the application of microbes, for instance, bacteria or fungi. This process can occur either directly by the activity of microbes or indirectly by metabolites produced by microbes (Vardanyan and Vyrides, 2019). Besides, bioleaching is considered as a sustainable purification method, which requires lower energy and cost in comparison to the non-biological processes (Zhao et al., 2019). However, bioleaching technique is typically slower than the conventional processes and the mechanism of iron reduction during bioleaching is still unclear.

Most studies have focused on the utilization of acid-producing microbes (such as *Bacillus* species and *Aspergillus niger*) and anaerobic iron respiration bacteria (such as *Shewanella* species) in bioleaching of kaolin. The study of Štyriaková et al. (2003) has demonstrated that *Bacillus* sp. was able to accelerate the dissolution of Fe from quartz sands by the production of organic acid and microbial colonization. In *Aspergillus niger,* it was shown that oxalic acid was far more effective than citric acid in complexing and dissolving iron content from a highly contaminated kaolin (Hosseini et al., 2007). In a bacterial iron-reduction experiment conducted by Zegeye et al. (2013), all strains of *Shewanella* sp. tested were capable to reduce iron impurities from industrial kaolin and able to improve whiteness index from 54% to 66%. Until now, majority of these studies have identified noticeable effect of the microbes towards the redox state of structural Fe, but the exact mechanism which underlying this process is still not completely understood. One of the mechanisms that was commonly reported is electron shuttle production, mostly observed in *Shewanella* species. This bacteria was shown to be capable of

transferring electrons to Fe(III) through the production of their own electron shuttles. This allows the insoluble Fe(III) reduced to soluble Fe(II) to happen without direct contact of the bacteria with the minerals (Pentráková et al., 2013). Nevertheless, most of the detailed mechanism of Fe reduction in the kaolin-water interface remains unclear especially the mechanisms which involves direct contact of microbes with the minerals.

Recent studies indicated that bacteria adhere onto the minerals surface via several interactions, such as formation of DLVO forces, hydrophobic interactions as well as secretion of extracellular polymeric substances (EPS) by bacterial cells (Flemming and Wingender, 2010; Ghashoghchi et al., 2017; Natarajan, 2018; Poorni and Natarajan, 2014, 2013; Tsuneda et al., 2003), and formation of cation bridges (Cao et al., 2011; Perdrial et al., 2009; Warr et al., 2009). These studies mentioned microbes-mineral interactions but mechanism in Fe reduction by microbes remains unclear. When bacterial cells adhere onto kaolin minerals, the cells aggregate at kaolin-water interfaces and produce EPS to form bacterial biofilms on kaolin surface. When there are more research about the molecular structures and the interactions between the responsible sites of the adhesive appendages of EPS and mineral surfaces, it is possible to develop new methods that can control biofilms formation and bacterial adhesion more effectively (Hori and Matsumoto, 2010).

In this research, indigenous *Bacillus* sp. strains isolated from kaolin procured from Bidor, Perak namely *Bacillus cereus*, *Bacillus aryabhattai* and *Bacillus megaterium* were used in the bioleaching process to determine their

efficiency in iron reduction. The variation of Fe concentration was determined by phenanthroline assay for every two days. Energy Dispersive X-Ray Spectroscopy (EDS) analysis was conducted to compare the chemical composition of elements between untreated (control) and treated (bioleached) samples. The changes of the glucose concentration and pH value in the medium were monitored at two days interval. The types and concentration of organic acids produced by the *Bacillus* sp. were detected and determined using Ion Chromatography. In addition, the morphological changes of the kaolin particles were observed using Scanning Electron Microscope (SEM). The modification of crystalline structure of kaolin before and after bioleaching process was examined by using X-Ray diffractometer (XRD). Furthermore, the formation of bonds and the electrical charges between the particles were studied using Fourier-Transform Infrared Spectroscopy (FTIR) and Zeta Potentiometer respectively. Based on these characterization analyses, the Fe reduction mechanisms in kaolin bioleaching were proposed.

1.2 Problem Statement of the Study

Recently, microbial leaching is increasingly favoured in removing metal impurities from low grade minerals due to its advantages of being environmentally friendly, low cost and less energy consumption. Therefore, bioleaching provides as an alternative to replace conventional treatments in removing iron from kaolin to increase its whiteness index. Based on previous studies, high iron reduction rates can be achieved without causing any significant changes to other mineral composition or crystalline structure of kaolin. Despite

4

this, bioleaching is a time consuming process as compared to conventional approaches and the mechanism of iron reduction in kaolin-water interface remains unclear. Other knowledge about the attachment of bacteria onto kaolin surface based on molecular level or atomic level included surface properties and bond formation are limited. Moreover, findings about the types of bacterial metabolites especially the metabolites concentration and also its effects on Fe^{2+}/Fe^{3+} ion equilibria in leaching process are still understudied. Hence, the goal of this study is to elucidate the iron reduction mechanism involving the microbe-minerals surface interactions. This knowledge will potentially assist in the development of an efficient and sustainable removal process of Fe impurities in kaolin.

1.3   Objectives:

The objectives of this study are:

i.   To determine the bioleaching efficiency of iron removal from kaolin by using *Bacillus cereus*, *Bacillus aryabhattai* and *Bacillus megaterium*.

ii.   To identify the types and concentrations of organic acids produced after the bioleaching process.

iii.   To analyse the changes in morphology and chemical composition of kaolin before and after bioleaching.

iv.   To elucidate the iron reduction mechanism of *Bacillus* sp. in bioleaching process.

CHAPTER 2

LITERATURE REVIEW

2.1   Kaolin

Kaolin clay, $Al_2Si_2O_5(OH)_4$ is a white and soft powder composed predominantly of mineral kaolinite and varying amounts of minerals such as feldspar and quartz (Kato et al., 2017; Kawanishi et al., 2020). It is the representative for 1:1 clay minerals which means its mineral structure composed of one tetrahedral sheet bound through apical oxygen atoms to one octahedral sheet (Neto et al., 2022; Uddin, 2018). Tetrahedral sheets mean Si^{4+} and Al^{3+} act as central atoms, which held by four oxygen atoms whereas Al^{3+}, Mg^{2+}, Fe^{3+} and Fe^{2+} act as central atoms, which held by six spanning oxygen or hydroxyls to form octahedral sheets (Mueller et al., 2014; Seredin et al., 2021).

Commercial kaolins are categorised as either primary or secondary. Primary kaolins are formed *in situ* by alternation of minerals such as weathering of crusts and soils (Adams et al., 2016). For example, feldspar, $KAlSi_3O_{10}$ and illite, $KAl_2(Si_3Al)O_{10}(OH)_2$ undergo chemical weathering and hydrolysed into kaolinite (eq 1,2). Besides, secondary kaolins refer to the kaolin transported from their origin of formation and remained as sediments which caused by the erosion

of plutonic rocks and hydrothermal fluids as well as low-grade metamorphic rocks (Galán, 2006).

$$2KAlSi_3O_{10} + 3H_2O \rightarrow Al_2Si_2O_5(OH_4) + 4SiO_2 + 2KOH \qquad (eq\ 1)$$

$$2KAl_2(Si_3Al)O_{10}(OH)_2 + 5H_2O \rightarrow Al_2Si_2O_5(OH)_4 + 4KOH \qquad (eq\ 2)$$
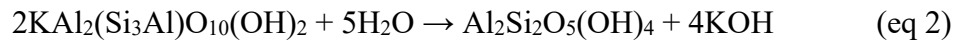
Kaolin is mined and widely used in many countries around the world. For example, Malaysia, China, Pakistan, Vietnam, Brazil, France and the United Kingdom (Neto et al., 2022). Kaolin is most applied in the paper coating and ceramics manufacturing industry (Bajpai, 2018; Rawski and Bhuiyan, 2017). It is also used as fillers in plastics and rubber compounds, as pigment additives in paints, and an essential resource in porcelain and pottery manufacturing (Hosseini and Ahmadi, 2015; Zegeye et al., 2013). Kaolin has high commercial value as it contributes for a wide range in manufacturing industry. However, the presence of iron oxides or oxyhydroxide will contaminate the kaolin as it will cause brownish or red colour developed in the finished products (Hajihoseini and Fakharpour, 2019). Thus, it will decrease the whiteness index and subsequently affect the quality of kaolin (Jing et al., 2021). Therefore, refinement of low-grade kaolin is needed to be studied and the technique of iron removal is refined over time to enhance the quality of kaolin (Fakharpour and Hajihoseini, 2021).

2.2   Physical and Chemical Treatments in Kaolin Leaching

Chemical leaching is the most common method employed by the kaolin industry to remove metal impurities using sodium hydrosulfite ($Na_2S_2O_4$), which also known as sodium dithionite (Zegeye et al., 2013). It commonly applied in removing colouring material such as iron oxides and titanium oxides without significantly affected the mineralogical characteristics of kaolin (Gougazeh, 2018). In laboratory test, chemical leaching is able to remove more than 90% of iron in kaolin giving a very small amount of iron concentration (below 0.3%) of product with high brightness value (above 94.0%), which meet the commercial specification (Thurlow, 2001). However, the chemical used is usually expensive and hazardous which needs proper storage and transport arrangements. The leaching process is also complicated as the parameters such as pH value, density of kaolin, oxygen content, and sodium hydrosulfite content required careful monitoring (Conley and Lloyd, 1970). Besides, high concentration of dissolved sulfates will be produced as waste so chemical treatment is required before disposal (Zegeye et al., 2013).

Besides chemical treatment, physical techniques also employed in the purification of clay minerals such as froth flotation, gravity separation, magnetic separation and reductive heating (Guo et al., 2010). Previously, high intensity of magnetic separation is a standard method used to remove iron and titanium impurities, thus improving the brightness of silicates (Štyriaková et al., 2003a). However, the impurities may tightly adsorbed or in a captured form. Thus it is not easy to be separated from clay minerals by physical methods (Lee et al.,

2002). Some of the machines are having complex operating conditions which require skilled workers to handle. Mirroring these shortcomings, conventional methods are generally expensive, require complex operating conditions and produce a high environmental impact (Asghari et al., 2013). Hence, the use of microorganisms has been a potential alternative to replace conventional methods in the leaching process.

2.3   Microbes in Kaolin Bioleaching

Microbial leaching is a simple and effective technique for extraction of metals impurities from low grade ore through the metabolism of microorganisms (Vardanyan and Vyrides, 2019). The processes are environmentally friendly as the interaction of microbes with clay minerals does not release hazardous wastes such as dissolved sulfates. It is also not energy intensive and low in operating cost (Hosseini and Ahmadi, 2015). There is a lot of Fe(III) reduction research, which involving wide variety of microbes such as *Shewanella* sp. (Liu et al., 2016; Zegeye et al., 2013), *Bacillus* sp. (Guo et al., 2010; Štyriaková et al., 2003b, 2003c), *Pseudomonas* sp. (Du et al., 2019), *Geobacter* sp. (Merino et al., 2020; Notini et al., 2019; Qiu et al., 2020), *Desulfitobacterium* sp. (Comensoli et al., 2017; Shelobolina et al., 2003), sulfate-reducing bacterium (Ikogou et al., 2017) as well as fungi such as *Aspergillus niger* (Hajihoseini and Fakharpour, 2019; Musiał et al., 2011).

These microorganisms are widely found in nature environment such as soils, sediments, sedimentary rocks and hydrothermal environments. High

abundance of such microorganisms in nature environments may be one of the reasons for industrial interest in removing Fe impurities from clay minerals. Since the microorganisms is naturally occurrence in environments, natural clay minerals such as kaolinite, illite and montmorillonite have no toxic effect towards bacterial cells (Jou and Nik Malek, 2016). However, the bacterial activity could be inhibited in the presence of antibacterial material which intercalated or adsorbed on them such as cetylpyridinium bromide and chlorhexidine acetate (Holešová et al., 2013). With such a broad of research, *Bacillus* sp., *Shewanella* sp. and *Aspergillus* sp. were chosen for further discussion as the representative of acid-producing bacteria, iron respiring bacteria and fungi respectively due to their commonly use in kaolin bioleaching study.

2.3.1   *Bacillus* sp.

Bacillus sp. is an acid-producing bacteria which reduces the pH of the their environment by producing corrosive acids and able to adapt under both aerobic or anaerobic conditions (Belyadi et al., 2019). Production of organic acids from *Bacillus* sp. is due to the by-products of their metabolism and the impact of this acidic metabolites is concentrated when they are confined at the biofilm or metal interface (Telegdi et al., 2018). This promotes the solubilisation of Fe impurities on kaolin when bacterial cells interact with minerals surface.

In Štyriaková et al. (1999), they have determined acetic, butyric, pyruvic, lactic, and formic acid as the product of metabolism during the cell growth of

Bacillus sp. Besides, Saeid et al. (2018) also studied the metabolites of *Bacillus* sp. (*B. cereus*, *B. megaterium* and *B. subtilis*). They have detected the presence of lactate, acetate, succinate, gluconate, and propionate during the bacterial growth. However, propionate was not detected in *B. megaterium*, while the concentration of lactate and acetate were the highest among these acids. The production of organic acids as metabolites in cell growth were able to solubilise and reduce the iron impurities contained in clay minerals.

2.3.2   *Shewanella* sp.

Shewanella sp. is an iron respiring bacteria which obtains energy when organic compounds or hydrogen is oxidised while ferric oxides is reduced under anaerobic condition (Ebrahiminezhad et al., 2017). In iron respiratory, hydrogen or organic compounds such as sugars and amino acids act as electron donors and oxidised to carbon dioxide while Fe(III) ions serve as the electron acceptor and reduced to soluble Fe(II) ions (Liu et al., 2017). During the electron transfer, bacterial cells secrete water soluble electron shuttles to transfer the electrons to electron acceptor without direct contact with the minerals (Bleam, 2012).

Zegeye et al. (2013) studied the iron reduction rate from kaolin using various types of *Shewanella* species which were *S. alga* BrY, *S. putrefaciens* CN32, *S. oneidensis* MR-1, and *S. putrefaciens* CIP 8040. Based on their results, the highest reduction rate was showed by *S. putrefaciens* CIP 8040 while the lowest showed by *S. putrefaciens* CN32. However, the final amount of total iron reduced after a five-day period was the same for both of these strains, inferred

that extent of reduction and reduction rate was not correlated. Furthermore, the research of Liu et al. (2017) proved the presence of humic acid was able to enhance the electron transfer and Fe(II) complexation of *S. oneidensis* MR-1 in reducing iron from Fe(III)-bearing clay minerals.

2.3.3 *Aspergillus* sp.

Aspergillus sp. is able to produce both organic and inorganic acids during bioleaching (Ghorbani et al., 2007). *Aspergillus* sp. which is a filamentous fungus able to remove metal impurities present in leaching solution, which called metal detoxification (Hosseini and Ahmadi, 2015). *A. niger* is commonly recognised to have oxalic acid as a product among the fungi of interest. Strasser et al. (1994) reported that oxalic acid can remove metals (aluminium, iron, lithium and manganese) efficiently from clay minerals. However, fungus is not recommend in industrial application since it is often produces toxin which could be a risk factor in the application as well as affecting the products quality (Štyriaková et al., 1999).

The study of Arslan and Bayat (2009) found *A. niger* was successful in removing iron impurities (77.13%) from kaolin after treated for 21 days at 30°C. Besides, Cameselle et al. (2003) performed a two-stage bioleaching process which *A. niger* was cultured in optimum conditions at the first stage. Then, the spent medium was used as the leaching medium at the second stage. By this, kaolin minerals with 80% whiteness index was achieved after leaching with *A. niger* medium for 5 hours at 45°C. This indicated that two-stage bioleaching is

more effective for fungus due to the existence of kaolin in growing cultures which affects adversely both fungus development and active metabolite production.

2.4 Attachment of Bacterial Cells on Minerals Surface

The bacterial cells either approach to mineral surface randomly or due to chemotaxis and motility, which allow the cells to move in a directed fashion (Chandraprabha and Natarajan, 2010). When bacterial cells reach crucial proximity to mineral surface within 1 nm, adhesion of bacterial cell on mineral surface depends on the electrical forces generated between two surfaces (Tsuneda et al., 2003). Mineral surface which are negatively charged will attract cations to be attached on the surface. The cations which have residual positive charges attract anions and double diffuse layers formed around minerals surface. This suppresses the adhesion of bacterial cells due to the electro-repulsive forces from the double diffuse layers. Nevertheless, the cell adhesion can be enhanced by extracellular polymeric substances (EPS) which is secreted by bacterial cells (Ghashoghchi et al., 2017).

EPS is mainly consists of polysaccharides as well as proteins, nucleic acids and lipids to form a complex combination of biopolymers (Khan et al., 2017). During the bacterial growth, EPS produced by bacterial cells construct the intercellular space of microbial accumulates and this forms the biofilm matrix, which is important for the growth and survival for microorganisms (van Hullebusch et al., 2003; Vu et al., 2009). During the bacterial cells adhere onto

mineral surface, the cells aggregate at kaolin-water interfaces and produce EPS to develop biofilms (Flemming and Wingender, 2010). Then the EPS adsorbs onto mineral surface through hydrogen bonding, which OH present in polysaccharides and/or the COOH present in both of polysaccharides or bacterial peptides binds with the Fe(III) on minerals (Selim and Rostom, 2018).

2.5   Summary

Many studies had proven the efficiency of microbial leaching in removing iron from kaolin minerals. Large amount of iron impurities on kaolin was reduced efficiently with high whiteness index of high-quality kaolin was achieved after microbial leaching. However, a detailed mechanism about Fe reduction from kaolin minerals by bacterial cell was rarely reported. Hence, this study determined the physicochemical properties and interaction between *Bacillus* sp. and kaolin minerals during bioleaching process. *Bacillus* sp. is more suited in laboratory test compared to other bacteria due to its versatility and flexibility to be grown in various conditions. Several of the unclear issues such as production of acids by *Bacillus* sp. and surface properties of kaolin with bacterial cells will be studied. Hence, the iron reduction mechanism of *Bacillus* sp. in kaolin bioleaching is clarified in this study.

CHAPTER 3

RESEARCH METHODOLOGY

3.1   Experimental Flowchart

Isolation and identification of bacteria from kaolin sample

Bioleaching of kaolin using identified bacteria for 10 days at 30°C at 250 rpm

Two day intervals (Day 0, 2, 4, 6, 8, and 10)

Before and after bioleaching (Day 0 and 10)

- Phenanthroline assay
- Glucose concentration
- pH measurement

- SEM-EDS
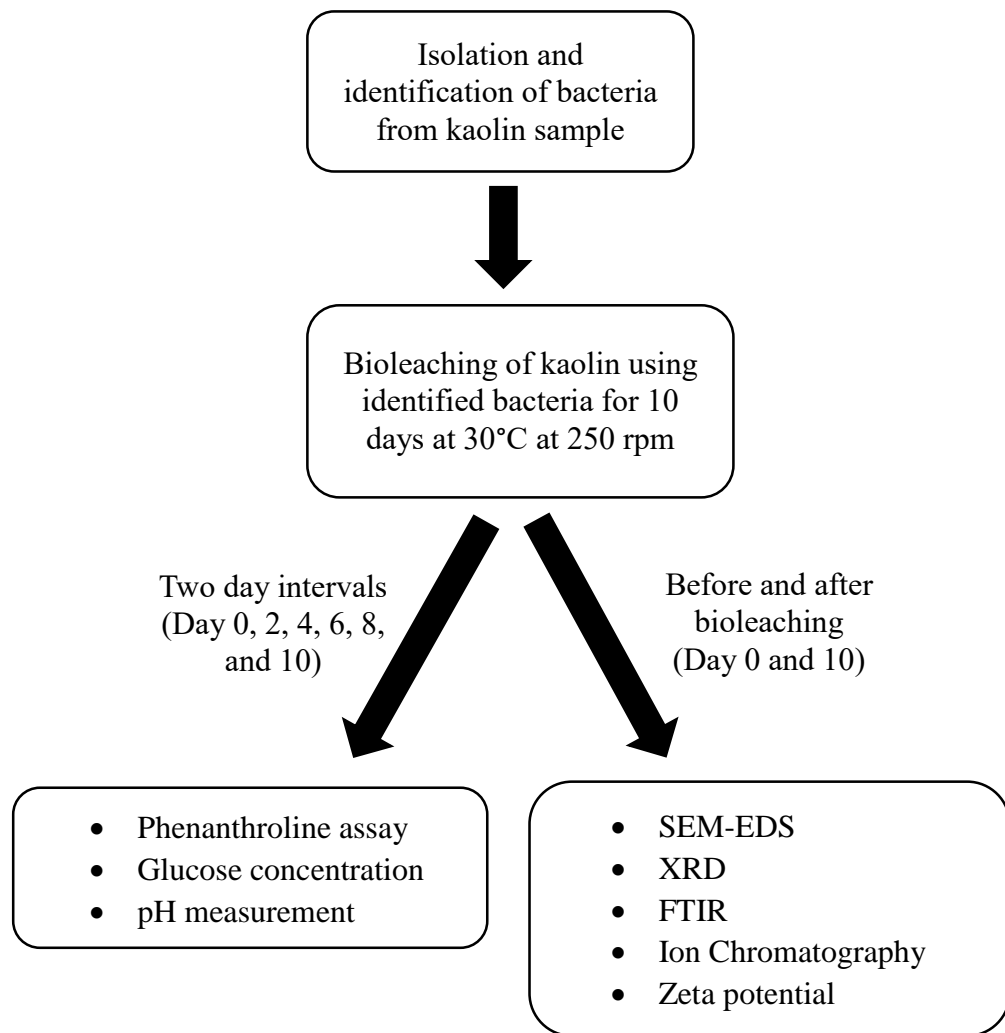- XRD
- FTIR
- Ion Chromatography
- Zeta potential

Figure 3.1: Flowchart of the experiments conducted

3.2   Kaolin Materials

Two pieces of wax paper were placed in the laminar flow hood and the kaolin cake was poured on the wax paper. The kaolin sample utilised in this study was supplied by Kaolin (M) Sdn Bhd (Perak, Malaysia). The pH of the kaolin was 4.0-5.5, with a brightness of 76-80% and average particles size of 2.5-3.5 µM. The kaolin cake was rolled into fine powder by using a roller and mixed for one hour to make sure it was homogenized. The kaolin powder was kept in a sterilized bottle and stored in dry place.

3.3   Isolation and Identification of Bacteria from Kaolin

Kaolin powder was mixed with sterile distilled water and diluted to 10 times dilution. The kaolin solution was transferred to LB agar by spread plate method and the plate was incubated overnight at 37°C. Subsequently, single colony with different physical appearances was isolated to a new agar plate respectively by streaking method and the plates were incubated overnight at 37°C. The single colony obtained was cloned into pCR 4-TOPO Vector and sent for 16S rRNA sequencing. The sequencing result was analysed by BLASTn (https://blast.ncbi.nlm.nih.gov/Blast.cgi) to identify the species of bacteria. Three of the bacteria samples were identified as *Bacillus cereus, Bacillus aryabhattai* and *Bacillus megaterium* respectively.

3.4 Bioleaching of Iron from Kaolin

Exactly 20 g of autoclaved kaolin powder was mixed with 200 mL of 10g/L glucose solution in 500 mL Erlenmeyer flask. The glucose solution acts as the nutrient source for bacterial cells during the bioleaching process (Guo et al., 2010). The concentration of 9 x 10^8 CFU of the identified bacteria was added into the kaolin solution respectively (Yong, 2019). The flask was incubated in an incubator shaker continuously for 10 days at 30°C with 250 rpm. The experiment was repeated with at least three biological replicates. Abiotic control sample was prepared in same approach as biotic samples, without the presence of bacteria.

3.5 Analysis of Sample

3.5.1 Phenanthroline Assay

Phenanthroline assay is a method to measure the Fe(III) reduction efficiency. Since Fe(III) is known to be reduced into Fe(II) in kaolin bioleaching process, Fe(II) concentration was measured at every two day intervals to observe the Fe(III) reduction efficiency up to 10 days.

To measure the Fe(II) concentration, 200 µL of 0.8% phenanthroline solution and 200 µL of 1.28 M ammonium acetate were mixed to form colorimetric reagent while 500 µL of 0.4 M sodium fluoride was used as complexing reagent. After the mixed solution was vortexed, 100 µL of sample was added and the solution was vortexed again. The solution was incubated in dark environment for 1 hour, three aliquots of 200 µL solution were transferred

17

to 96-well microtiter plate and analysed by using ELISA microplate reader (Tecan, Switzerland) (Figure 3.2) at wavelength of 492 nm. The standard curve for phenanthroline assay was done between 0-10 µg/mL of Fe(II) concentration with R^2 value of 0.9977 and equation $y = 0.01x$ was obtained, which y represents absorbance value while x represents Fe(II) concentration (Figure 3.3).
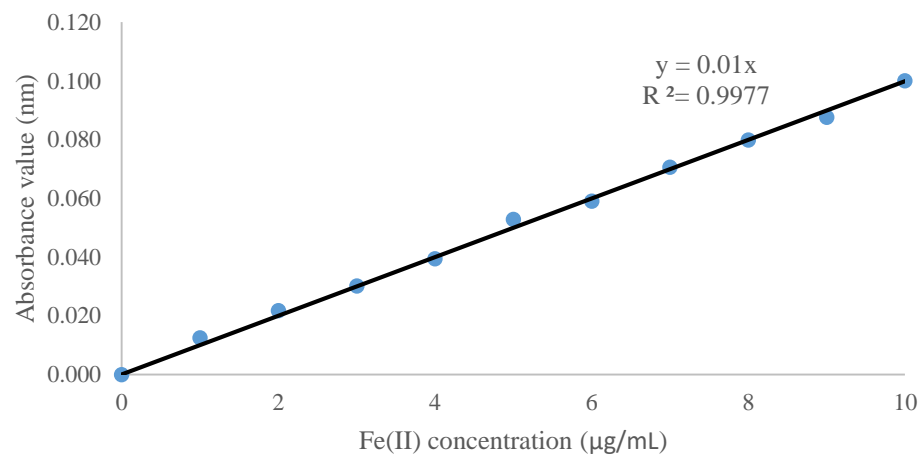

Figure 3.2: ELISA microplate reader (Tecan, Sunrise^{TM})

Figure 3.3: Standard curve for phenanthroline assay

3.5.2 Energy Dispersive X-Ray Spectroscopy (EDS)

EDS (Hitachi, Japan) (Figure 3.4) is a microchemical analysis technique used in conjunction with SEM. The mineral composition of the kaolin such as O, K, Al and Fe was analysed before and after the experiment. In EDS analysis, bioleaching efficiency was calculated by the changes of Fe composition before

18

and after bioleaching.

$$\text{Bioleaching efficiency (\%)} = \left(\frac{X_i - X_f}{X_i}\right) \times 100\%$$

X_i = weight percentage (wt %) of Fe composition in kaolin before bioleaching

X_f = weight percentage (wt %) of Fe composition in kaolin after bioleaching

3.5.3 Scanning Electron Microscope (SEM)

The effect of iron removal on the morphology change of kaolin was observed by using SEM (Hitachi, Japan) (Figure 3.4). The dried kaolin samples was coated with gold prior to the analysis. The morphology changes of kaolin was analysed before and after the experiment. At least three images were taken for each of the sample.

Figure 3.4: SEM-EDS (Hitachi, S-3400N)

3.5.4 X-Ray Diffraction (XRD)

XRD (Shimadzu, Japan) (Figure 3.5) is an analysis technique to determine the crystalline structure of the kaolin particles before and after bioleaching process. The kaolin sample was placed into sample holder and analysed by using X-ray diffractometer. The XRD patterns were gathered over a scale of 10° to 80° 2θ applying Cu Kα radiation (40 kV, 40 mA), with a 0.05°

19

step width and a nominal collecting time of 30 seconds per 0.1°. The XRD pattern of the treated samples were compared with the untreated sample to analyse the effect of bioleaching on the changes of structural modification of the kaolinite.

Figure 3.5: XRD (Shimadzu, XRD6000)

3.5.5 Monitoring of Glucose Concentration

In this study, glucose concentration was measured at two-day intervals to monitor the change of glucose concentration during bioleaching. Glucose solution acts as the carbon source for bacteria to obtain energy for metabolism. This means metabolism of bacteria will be affected during the lacks of energy source and henceforward decrease the efficiency of iron removal (Lempp et al., 2020).

The concentration of glucose in kaolin solution was measured by treating the samples with dinitrosalicylic acid (DNS) reagent in 1:1 ratio and the solution was heated at 100°C for 5 minutes. After 5 minutes, the tubes were cooled in ice immediately and 5 mL of distilled water was added. Following this, the tubes were vortexed, and the absorbance value of the solutions was read at 540 nm by

spectrophotometer (Thermo Fisher Scientific, USA) (Figure 3.6). The standard curve for glucose concentration analysis was done at 0-10 g/L of glucose concentration with R^2 value of 0.9598 and equation of $y = 0.3696x$ was obtained, which y represents absorbance value while x represents glucose concentration (Figure 3.7).

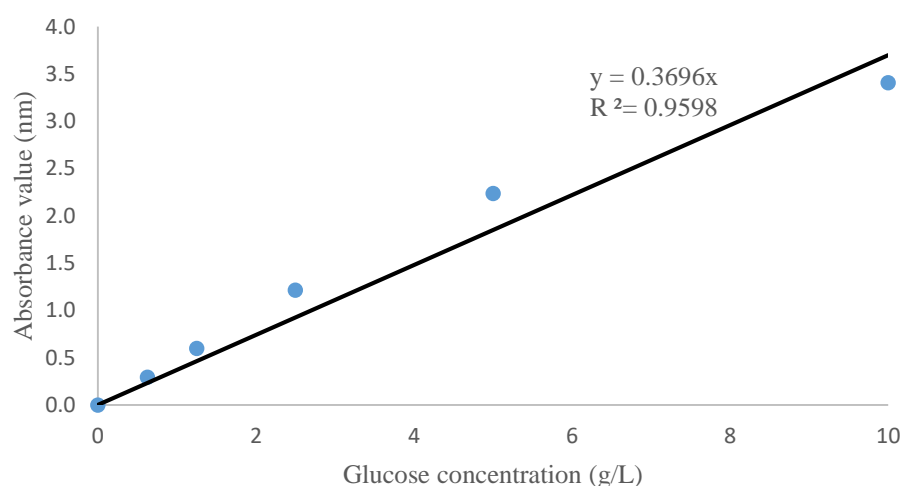Figure 3.6: Spectrophotometer (Thermo Fisher Scientific, NanoDrop 2000c)

Figure 3.7: Standard curve for glucose concentration analysis

3.5.6 Ion Chromatography

Ion chromatography (Metrohm, Switzerland) (Figure 3.8) was used in this study to identify the type and concentration of organic acids produced by bacterial cells. This analysis was conducted before and after bioleaching process to clarify the type and concentration of the acid production by *Bacillus* species

when in contact with kaolin. Sulfuric acid eluent (1 L) was prepared by mixing 0.5 mmol/L sulfuric acid with 15% acetone. Deionized water was added to the eluent and the mixture is then vacuum-filtered through a 0.2 µm nylon filter.

Figure 3.8: Ion chromatography (Metrohm, Metrosep Organic Acids-250/7.8)

Standard substances of the acids were purchased from Sigma-Aldrich (St. Louis, MO, USA). All the standard and samples solution were diluted with deionised water and filtered through 0.2 µm membrane filter before injection into ion chromatography. The analysis was conducted using 0.5 mL/min flow rate with 5 MPa of maximum pressure. The injection volume was 20 µL. All of the measurements were taken at least three technical replicates. Figure 3.9(a), (b), (c), (d) and (e) show the standard curve for malic, acetic, formic, succinic, and lactic acid respectively. All standard curves achieved the R^2 value of above 0.9 whereas the equations obtained were used to measure the concentration of organic acids respectively.
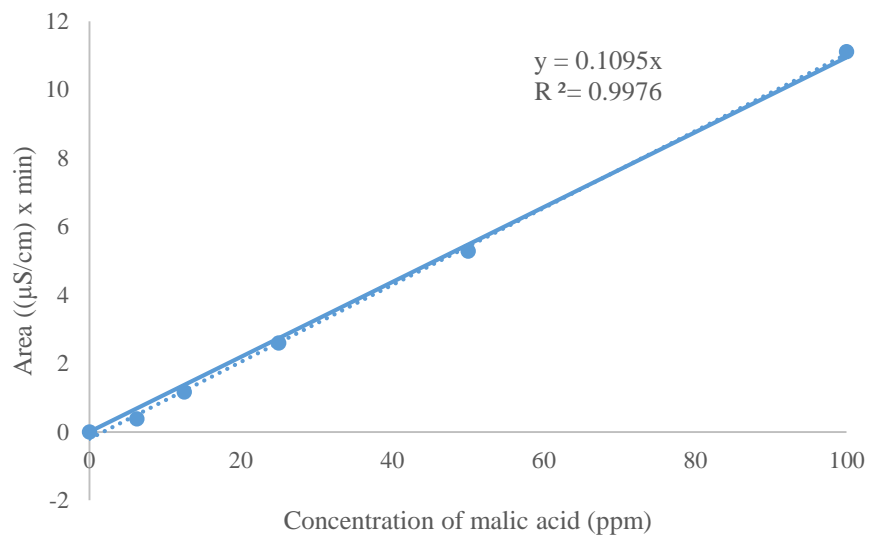
Figure 3.9(a): Standard curve for detection of malic acid concentration
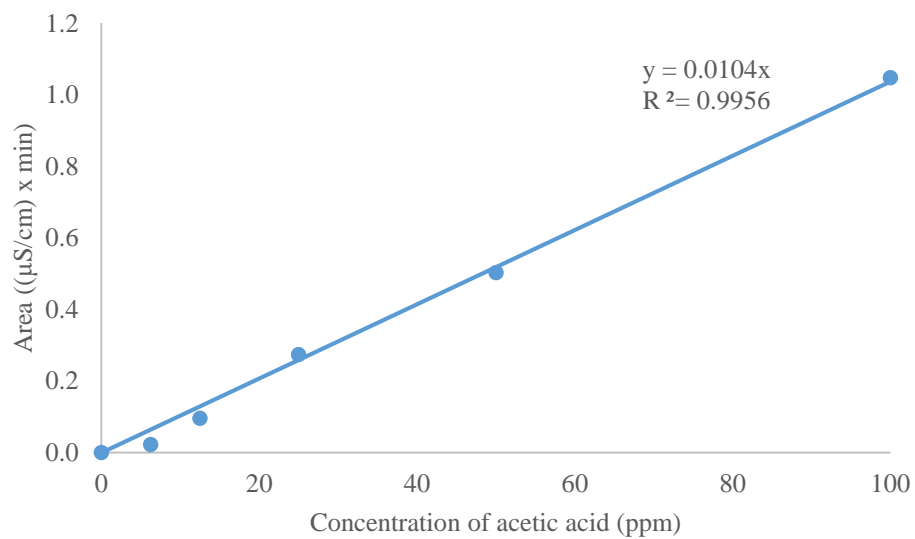

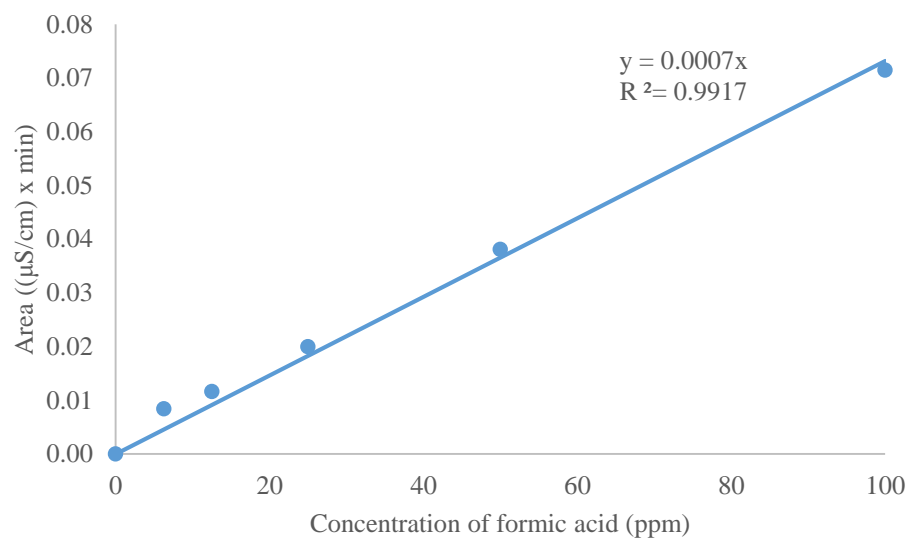Figure 3.9(b): Standard curve for detection of acetic acid concentration

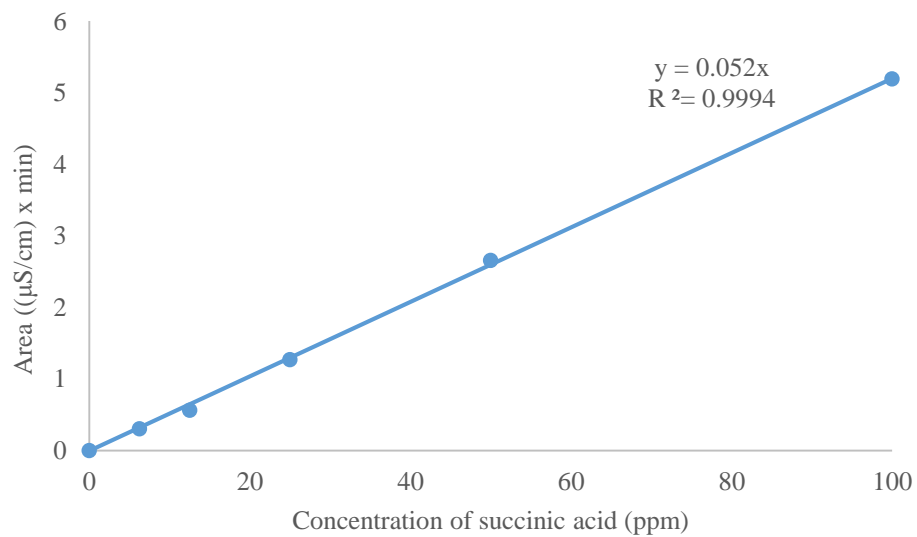Figure 3.9(c): Standard curve for detection of formic acid concentration

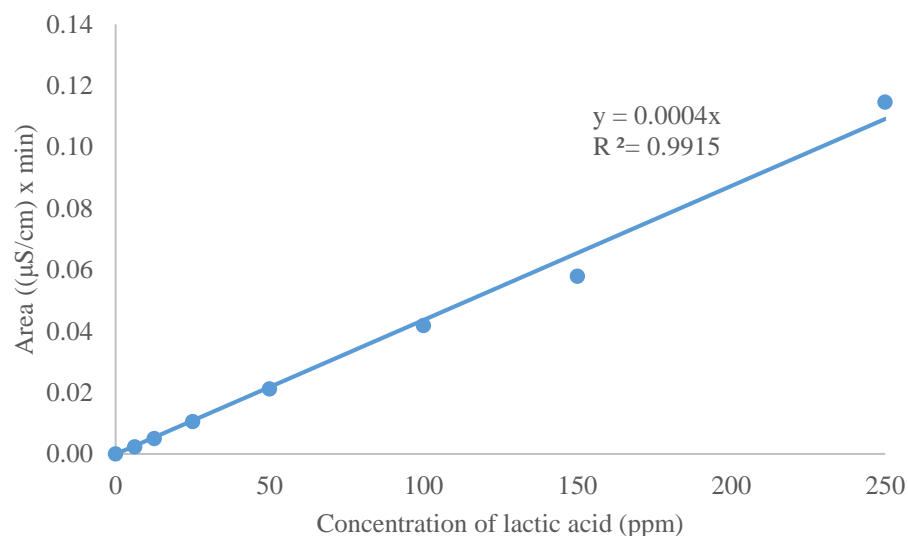Figure 3.9(d): Standard curve for detection of succinic acid concentration

Figure 3.9(e): Standard curve for detection of lactic acid concentration

3.5.7 Fourier-Transform Infrared Spectroscopy (FTIR)

FTIR is a equipment used to determine the bond formation between the mineral surface and bacteria during bioleaching process. The dried treated sample was placed on the sample holder of FTIR (Thermo Fisher Scientific, USA) (Figure 3.10) to record the infrared absorption spectra. Since the organic structure of bacteria composed mainly of polysaccharides and lipids (protein), this analysis also determine the adsorption of bacteria onto the Fe(III) on surface of mineral via the OH present polysaccharides and/or the COOH present in both of the polysaccharides or bacterial peptides. The formation of hydrogen bond, if any, will allow us to elucidate the attachment mechanism of the bacteria cell onto the kaolin particles.

Figure 3.10: FTIR (Nicolet, IS10)

3.5.8 Zeta Potential

Zeta potential is the potential difference and used to measure the electrical charge of the particles. When the value is higher, the colloid dispersion is more stable. By measuring the value of zeta potential, surface properties between bacteria and kaolin in bioleaching can be determined. The sample was measured at five-day intervals and the sample was vortexed well before analysed by the zeta potentiometer (Malvern, UK) (Figure 3.11). The measurement of *Bacillus sp.* and the kaolin samples in absence or presence of bacteria will be performed. These measurements can help to explain how the bacteria cell and kaolin particles approach one another, the presence of oppositely charged surfaces and the charge neutralization, if observed may indicate the role of electrostatic forces in the contact between the kaolin particle and bacteria cell.

Figure 3.11: Zeta potentiometer (Malvern, Zetasizer Nano-ZS)

CHAPTER 4

RESULTS AND DISCUSSION

4.1   Fe Reduction in Kaolin Bioleaching by *Bacillus* sp.

During the bioleaching process, insoluble Fe(III) in kaolin sample will reduced to soluble Fe(II) (Zegeye et al., 2013). This means the removal of Fe(III) will lead to the increasing Fe(II) concentration in solution. Hence, the sample with higher Fe(II) concentration infers that the efficiency of Fe(III) removal is also higher. In this work, the Fe(II) concentration was measured using the quantitative spectrophotometric determination of Fe(II) by o-phenanthroline (Herrera et al., 1989).

Based on the phenanthroline assay measurements taken during bioleaching (Figure 4.1), all samples showed increasing trends in Fe(III) reduction up until day 6-8 followed by a slight decrease towards the end of the 10 day period. In abiotic control, the concentration of Fe(II) increased slowly and constantly from 0.18 μg/mL at day 0 to 0.50 μg/mL at day 8. It then decreased to 0.25 μg/mL at day 10. For kaolin treated with *B. cereus*, the amount of reduced Fe(II) increased from 0.19 μg/mL to 0.54 μg/mL from day 0 to day 2. Next, the Fe(II) amount increased slightly to 0.57 μg/mL at day 4 then it increased significantly and reached the highest peak at day 8, which is

1.43 µg/mL of Fe(II) in solution. From day 8 to day 10, the concentration reduced from 1.43 µg/mL to 0.92 µg/mL.

Both of the kaolin solution bioleached with *B. aryabhattai* and *B. megaterium* had the initial Fe(II) concentration of 0.14 µg/mL and 0.24 µg/mL, respectively. For the kaolin treated with *B. aryabhattai*, Fe(II) concentration increased gradually to 0.51 µg/mL at day 4 and rose to 1.26 µg/mL at day 6. After day 6, the efficiency of Fe(III) reduction was decreased and 0.95 µg/mL of Fe(II) was detected at day 10. Fe(III) reduction for kaolin treated with *B. megaterium* showed a linear increment to 0.70 µg/mL at day 4, reaching the highest peak at day 6 where 1.25 µg/mL of Fe(II) concentration. Then, the concentration dropped steadily to 0.81 µg/mL at day 10.
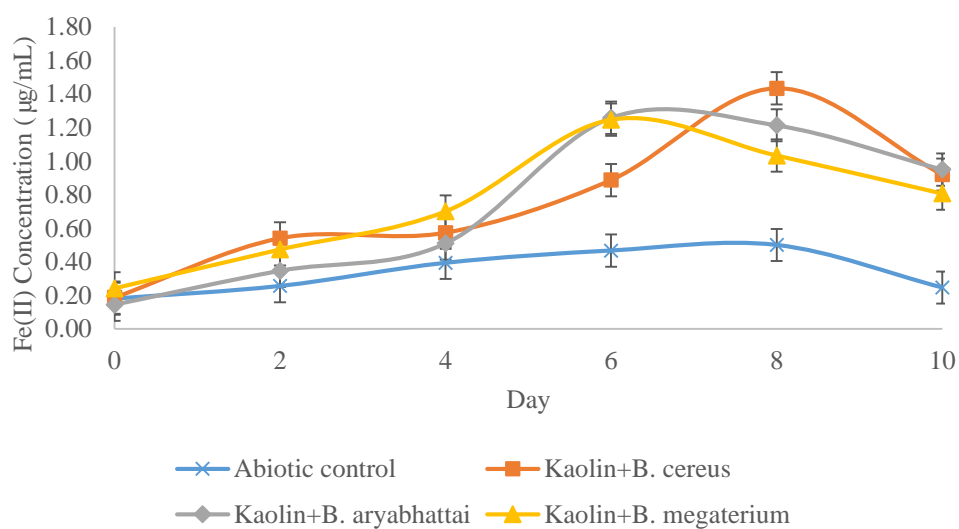

Figure 4.1: Fe(II) concentration in kaolin bioleaching with and without bacteria. The amount of Fe(II) measured infers to the amount of Fe(III) reduced. (Vertical bars shown in line graph represent the pooled standard deviation.)

The results of phenanthroline assay revealed that the presence of bacteria is synonymous with increased concentrations of Fe(II) in solution for all three

species of *Bacillus* compared to the abiotic control during the 10-day period. All of the tested *Bacillus* sp. were capable to reduce Fe(III) in kaolin and there was not any significant Fe(II) concentration observed in abiotic (control) samples. This infers that the presence of Fe(II) observed in samples treated with bacteria is linked to the presence of bacteria. However, the efficiency of Fe(III) reduction was decreased after the peak either on day 6 or day 8. One plausible explanation for this decrease is the acidification of the glucose solution which affected the microbial viability of the species present and resulted in decreased bioleaching efficiencies (Bonora et al., 2012).

The comparison of chemical composition of elements in raw sample with treated samples is analysed using EDS analysis and results are shown in Table 4.1. The chemical composition of elements such as O, Al, Si and K exhibited slight difference before and after leaching process. However, the chemical composition of Fe were notably decreased in all treated samples. Bioleaching efficiency of treated samples is calculated by the changes of Fe composition before and after bioleaching which mentioned in section 3.4.2.

Based on the EDS results, abiotic control had the lowest bioleaching efficiency which is 3.57% while kaolin treated with *B. cereus* had the highest which is 43.86%. The samples treated with *B. aryabhattai* and *B. megaterium* showed the bioleaching efficiencies of 13.57% and 8.43% respectively. This suggested that *Bacillus* sp. selectively reduced Fe from kaolin in leaching process without affecting much on the chemical composition of other elements. The significant difference of bioleaching efficiency observed between bio-

treated samples and abiotic control proved the potential of *Bacillus* sp. in improving the Fe(III) removal efficiency.

Table 4.1: Weight percentage of elements in kaolin after bioleaching

Elements	wt%				
	Raw kaolin	Abiotic control	Kaolin treated with *B. cereus*	Kaolin treated with *B. aryabhattai*	Kaolin treated with *B. megaterium*
O	48.62	49.36	47.79	48.99	49.90
Al	20.06	19.74	20.29	20.30	19.35
Si	25.67	25.43	26.78	25.85	25.13
K	3.91	3.79	3.58	3.35	4.02
Fe	1.75	1.69	0.98	1.51	1.60
Bioleaching efficiency (%)		3.57 ±0.06	43.86 ±0.29	13.57 ±0.05	8.43 ±0.11

The results of both phenanthroline assay and EDS analysis showed the Fe(III) reduction and bioleaching efficiency in sample treated with *Bacillus* sp. were notably elevated compared with results from the abiotic control. This infers that the presence of bacterial cells is closely linked to the reduction efficiency of Fe(III) to Fe(II). While Fe(II) concentration measured using the phenanthroline method (Figure 4.1) appears to unanimously show a predominantly increasing trend up until day 6-8, with most of the concentrations to be not far from each other regardless of *Bacillus* species, EDS results in Table 4.1 tells a slightly different story. Bioleaching efficiencies from the EDS range from 8.43% to 43.86%. This larger discrepancy of efficiencies between species could be due to the characterisation method itself. Between the EDS and phenanthroline assay, phenanthroline assay typically has lesser margin of errors since it is a chemical technique. However, EDS analysis depends on where the SEM image is taken where the readings only represent the Fe concentration of local sites but not the

entire sample. This is because the natural occurrence of ferric hydroxide impurities on kaolin surface is expected to be mostly not uniform and scattered in varying concentrations across the kaolin surface. Hence, average readings from four sites of Fe concentration were measured for each sample to provide a better indication of Fe concentration but phenanthroline results are expected to be more accurate and precise.

4.2   Mineralogical Analyses of Kaolin in Bioleaching

The surface morphology of kaolin particles before and after bioleaching was investigated through SEM analysis. Figure 4.2 shows raw kaolin particles before leaching in amorphous structure. They exhibited varying size and thickness. Examination of the images shows that the edges of the particles were smooth and round-shaped.
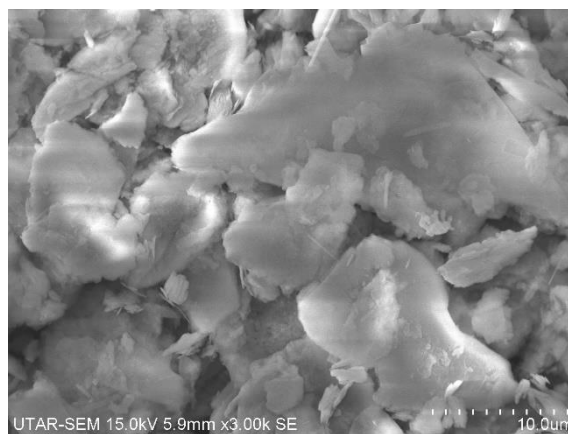

Figure 4.2: SEM images for morphology of raw kaolin particles under magnification of 3000x shows the edges of the particles were smooth and round-shaped.

Table 4.2 shows the images of kaolin particles for the abiotic control sample as well as samples exposed to all three species of *Bacillus* respectively.

31

For all three species, SEM images of kaolin surface after bioleaching revealed edges of the particles that appear visibly sharper and slightly damaged or chipped. By comparing the images of the abiotic control sample with those of the raw sample (Figure 4.2), it is observed that the kaolin particles in abiotic control sample after leaching had no significant morphological changes observed, suggesting that the changes in kaolin surface morphology in the sample with bacteria were caused by the bacterial interaction with kaolin surfaces.

While SEM analysis suggests bacterial cells damaged the kaolin particles, XRD results indicated that there was very little (if any) structural modification in kaolinite during the bioleaching for all three species respectively. In the XRD results, kaolin treated with *Bacillus* sp. for 10 days at 30 °C showed similar pattern with untreated kaolin (Figure 4.3(a), (b), (c)). Furthermore, the results show that there was no evidence of secondary mineral phases formation for all three species after bioleaching.
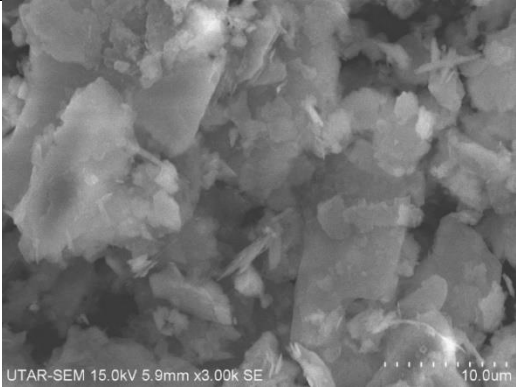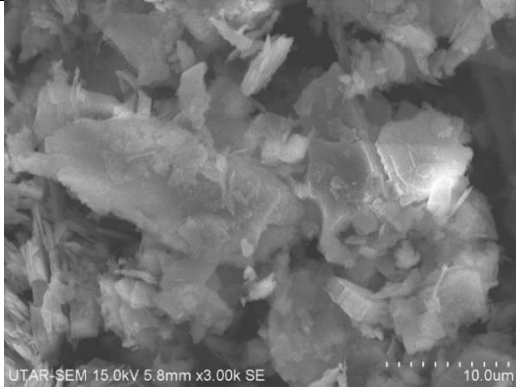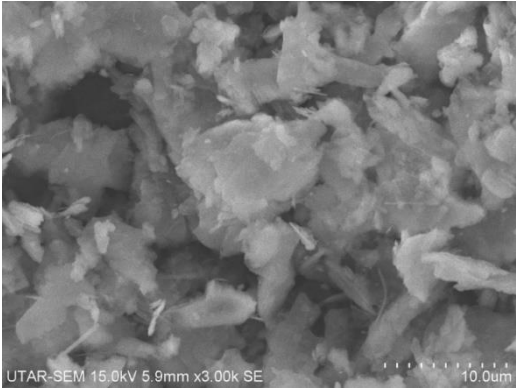
In addition, FTIR measurement were taken to study the bond formation during the attachment of bacterial cells onto kaolin surfaces. Figure 4.4(a), (b) and (c) show FTIR results for kaolin before and after treatment with *B. cereus*, *B. aryabhattai* and *B. megaterium,* respectively. The comparison of FTIR results for kaolin after treatment with all three *Bacillus* sp. is shown in Figure 4.4(d). In all of the results, there was a peak at 3675 cm^{-1} indicating there was existence of O-H bands (Selim and Rostom, 2018). This hydroxyl band is inferred to have originated from the polysaccharide portion of the bacteria structure. Adsorption of *Bacillus* sp. onto kaolin surface may have taken place onto positive Fe(III)

sites through the OH (polysaccharide portion of bacteria) (Abdel-Khalek et al., 2013).

From a morphological perspective, the interaction of bacterial cells with kaolin caused the slight damage to the edges of the kaolin particles (Table 4.2). Observations of SEM images infer that the treated kaolin has the particles with highly crystalline structure compared to the untreated kaolin which exhibits in amorphous structure. This observation is in agreement with Štyriaková and Štyriak (2000), which the SEM analysis showed the surface of kaolin particles were destroyed by *Bacillus* sp. after treated for 3 months at 28°C.

However, XRD analysis indicated that there was just very little (if any) of structural modification in kaolinite as well as, absence of secondary mineral phases development after bioleaching. Previous work by Zegeye et al. (2013) shows similar findings where, there was an absence of secondary mineral and crystal-chemical alternation of kaolin in the samples after bioleached by *Shewanella* sp. for 5 days at 30°C. Hence, while the species employed in our experiments differ from those of Zegeye et al. (2013), SEM and XRD analysis conducted in this work showed bacterial cells slightly damaging the surface and edges of the kaolin without causing structural changes.

Table 4.2: Morphology of kaolin particle before and after bioleaching under magnification of 3000x. The edges of the particles after bioleached with bacteria appear visibly sharper and slightly damaged or chipped.

Samples	Before bioleaching	After bioleaching
Abiotic control		
Kaolin treated with *B. cereus*		

Kaolin treated with
B. aryabhattai
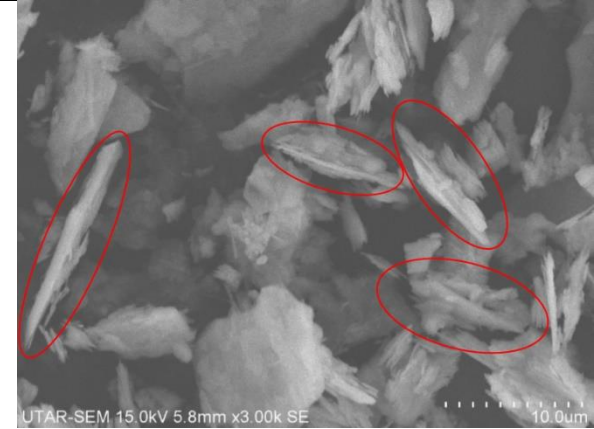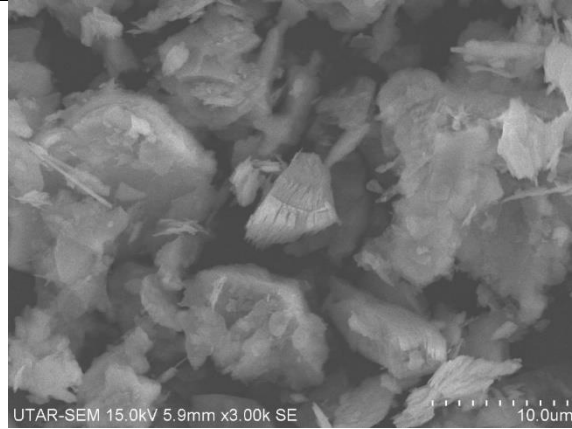
Kaolin treated with
B. megaterium
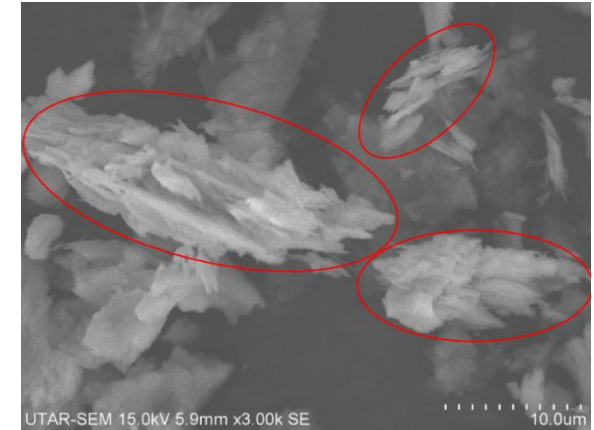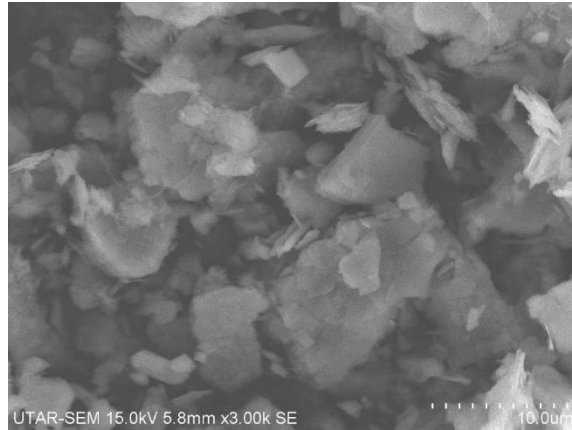
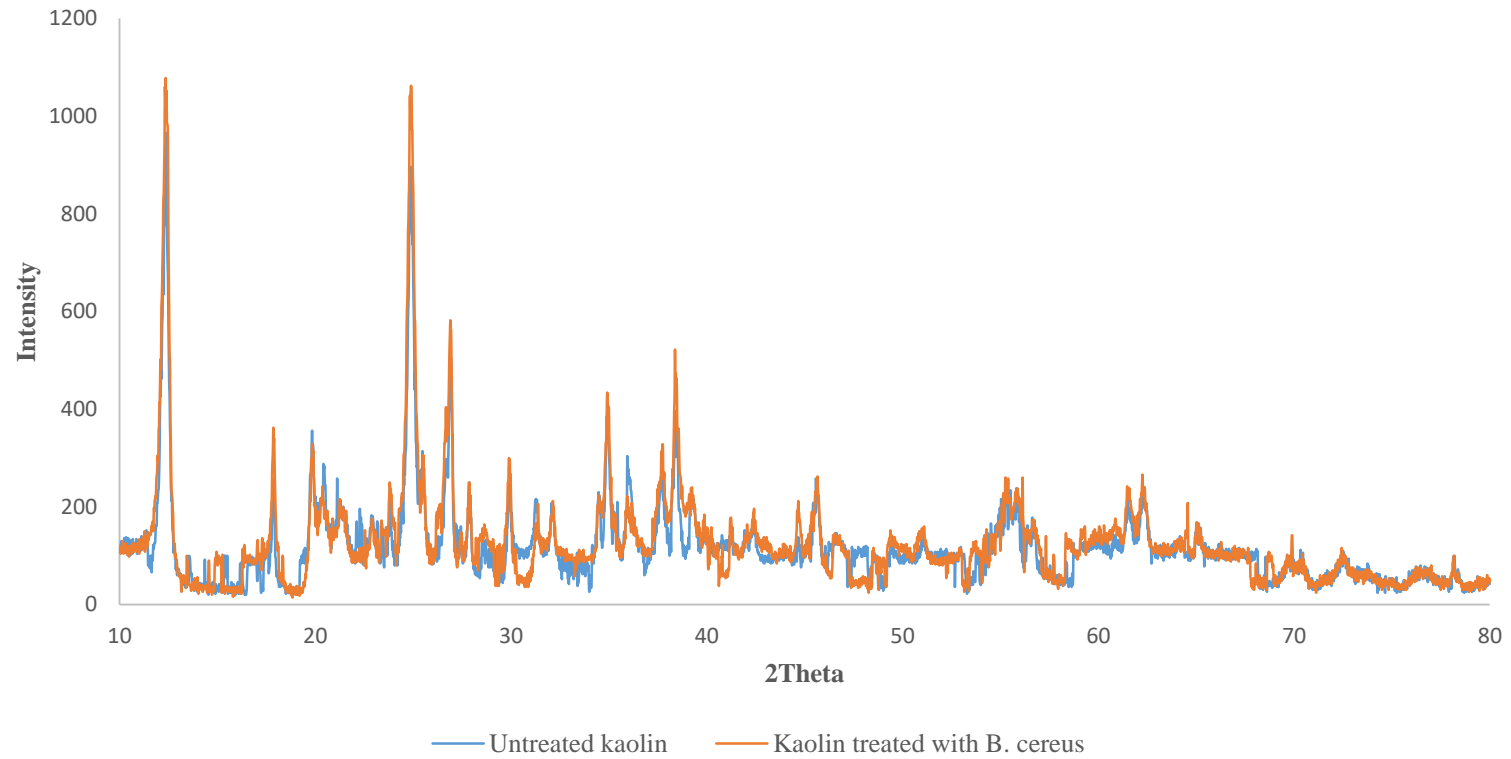Figure 4.3(a): XRD patterns of kaolin before and after bioleached with *B. cereus*. Results showed kaolin treated with *B. cereus* for 10 days at 30 °C showed similar pattern with untreated kaolin.

Figure 4.3(b): XRD patterns of kaolin before and after bioleached with *B. aryabhattai*. Results showed kaolin treated with *B. aryabhattai* for 10 days at 30 °C showed similar pattern with untreated kaolin.
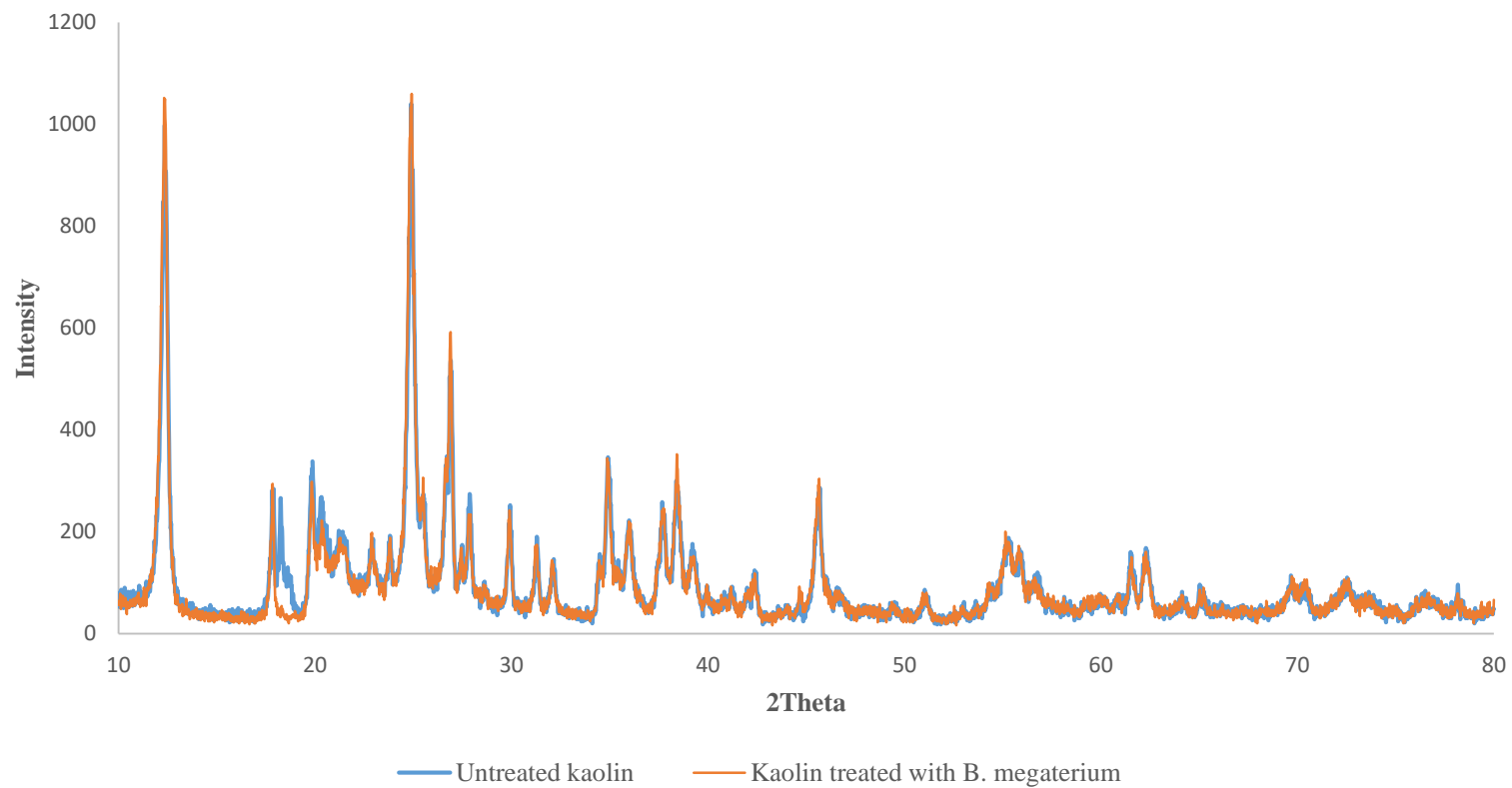
Figure 4.3(c): XRD patterns of kaolin before and after bioleached with *B. megaterium*. Results showed kaolin treated with *B. megaterium* for 10 days at 30 °C showed similar pattern with untreated kaolin.
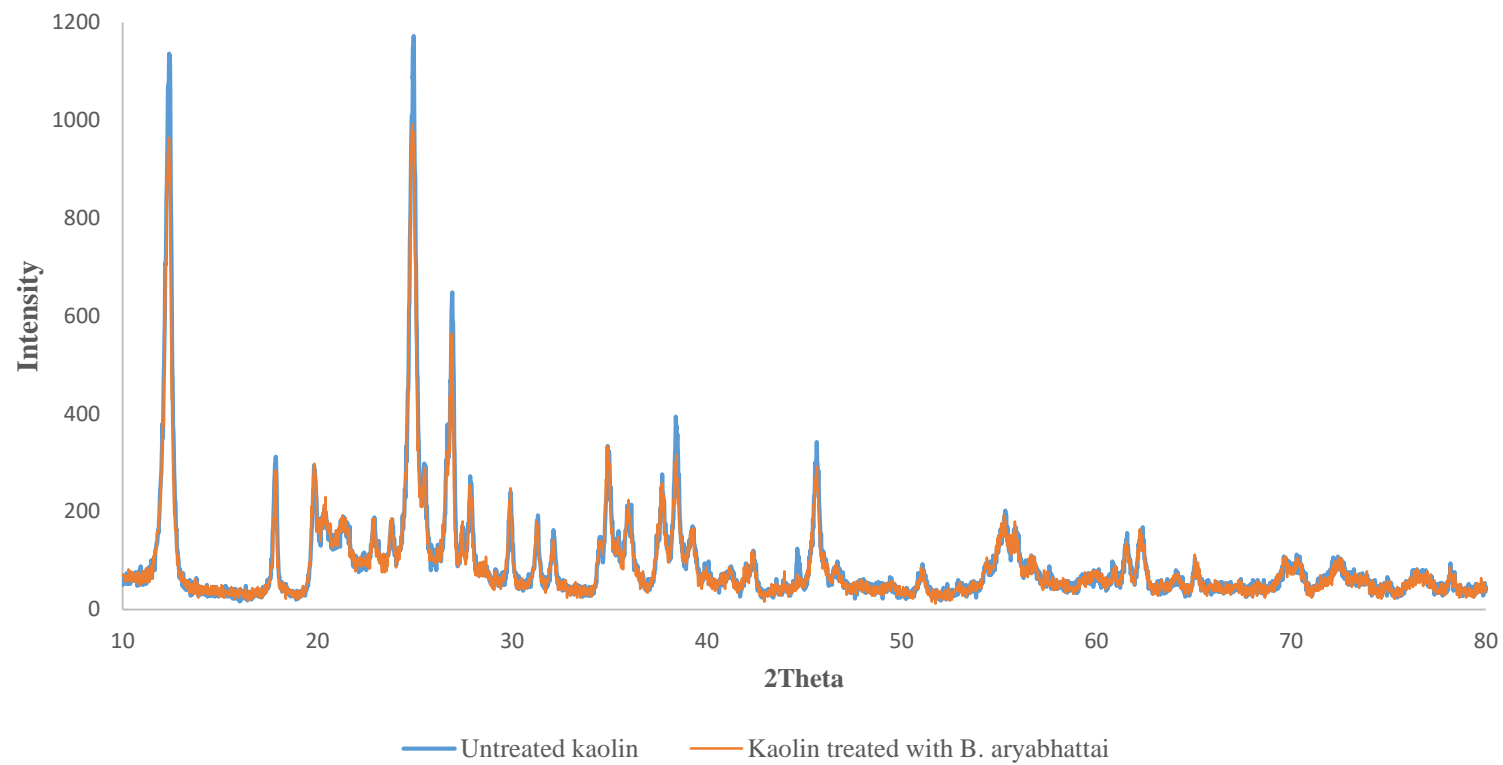
Figure 4.4(a): FTIR for kaolin before and after bioleached with *B. cereus*. There was a peak at 3675 cm-1 indicating the existence of O-H bands.

Figure 4.4(b): FTIR for kaolin before and after bioleached with *B. aryabhattai*. There was a peak at 3675 cm-1 indicating the existence of O-H bands.
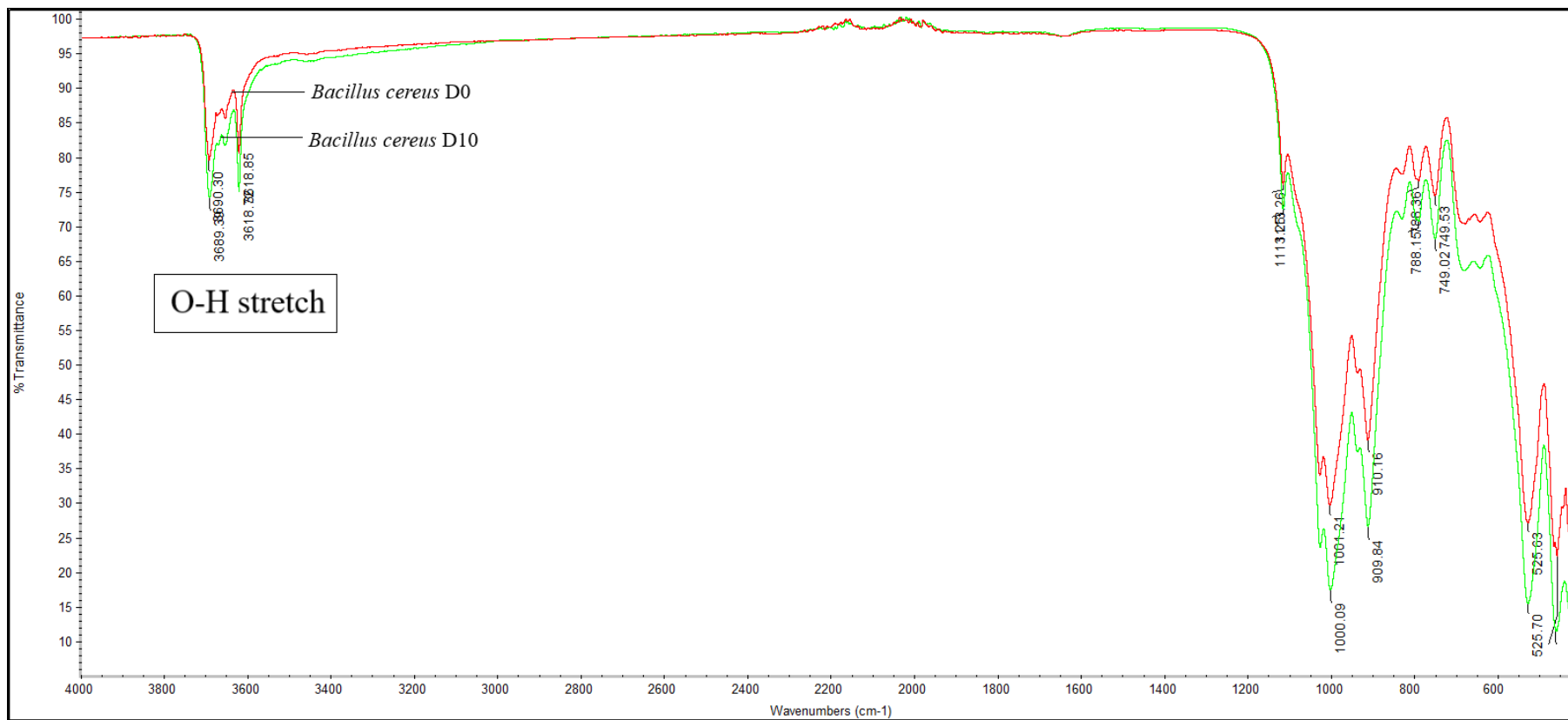
Figure 4.4(c): FTIR for kaolin before and after bioleached with *B. megaterium*. There was a peak at 3675 cm-1 indicating the existence of O-H bands.
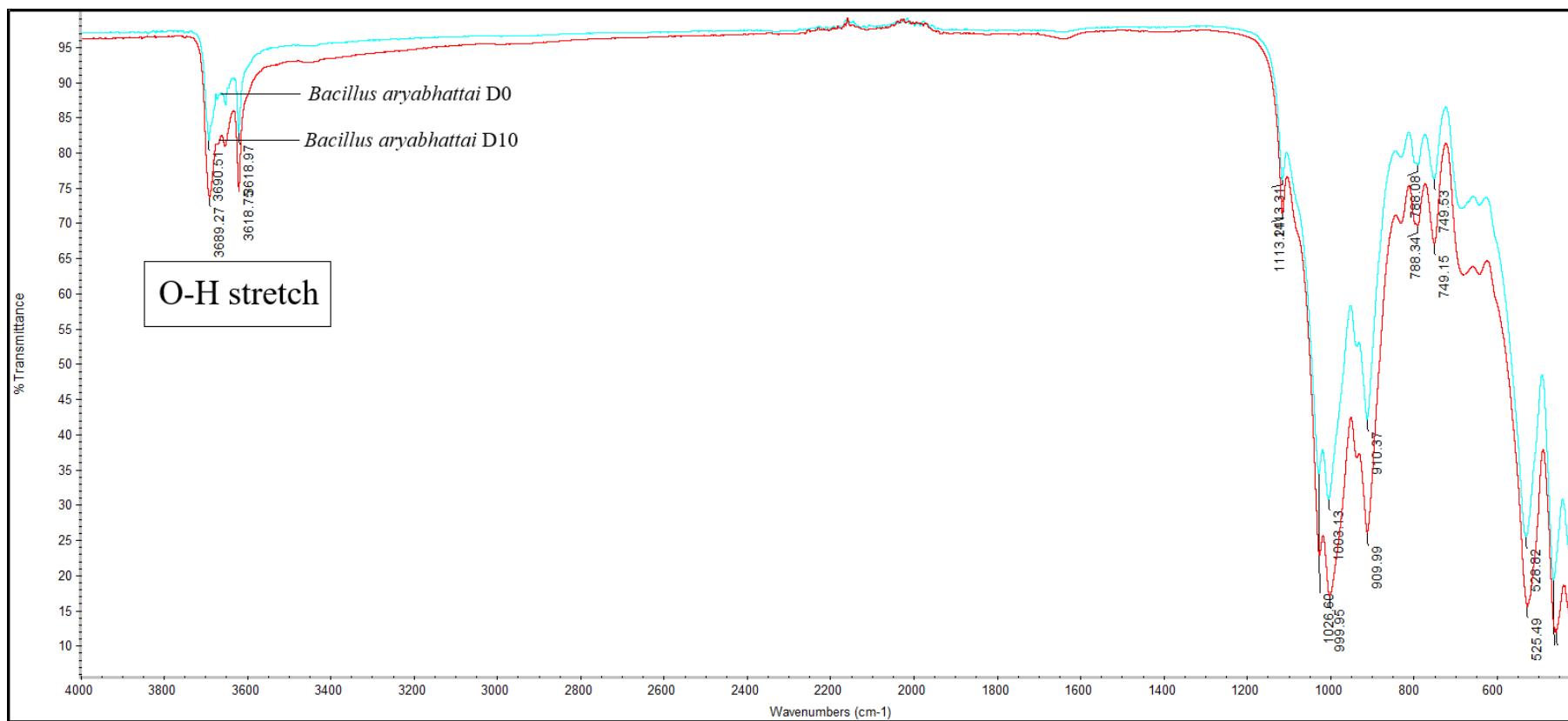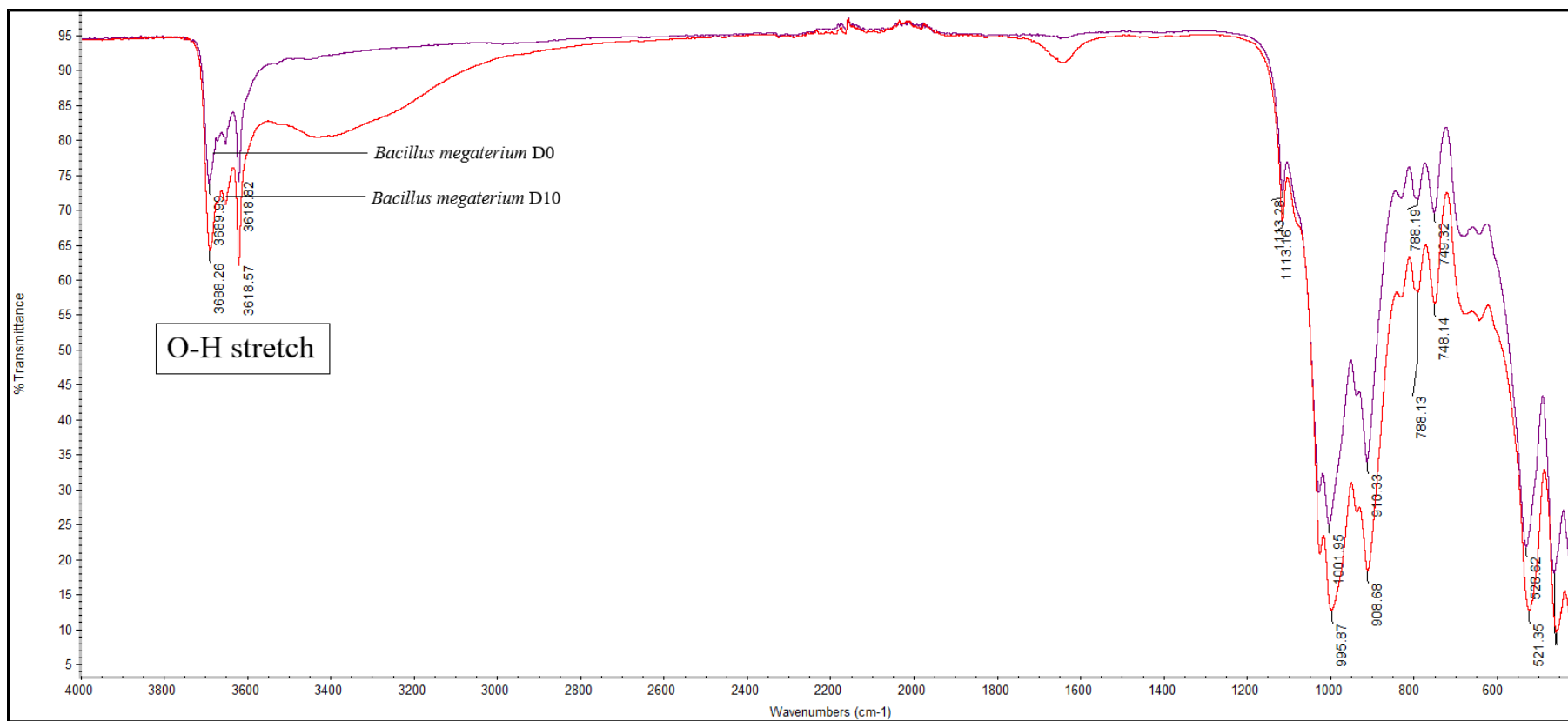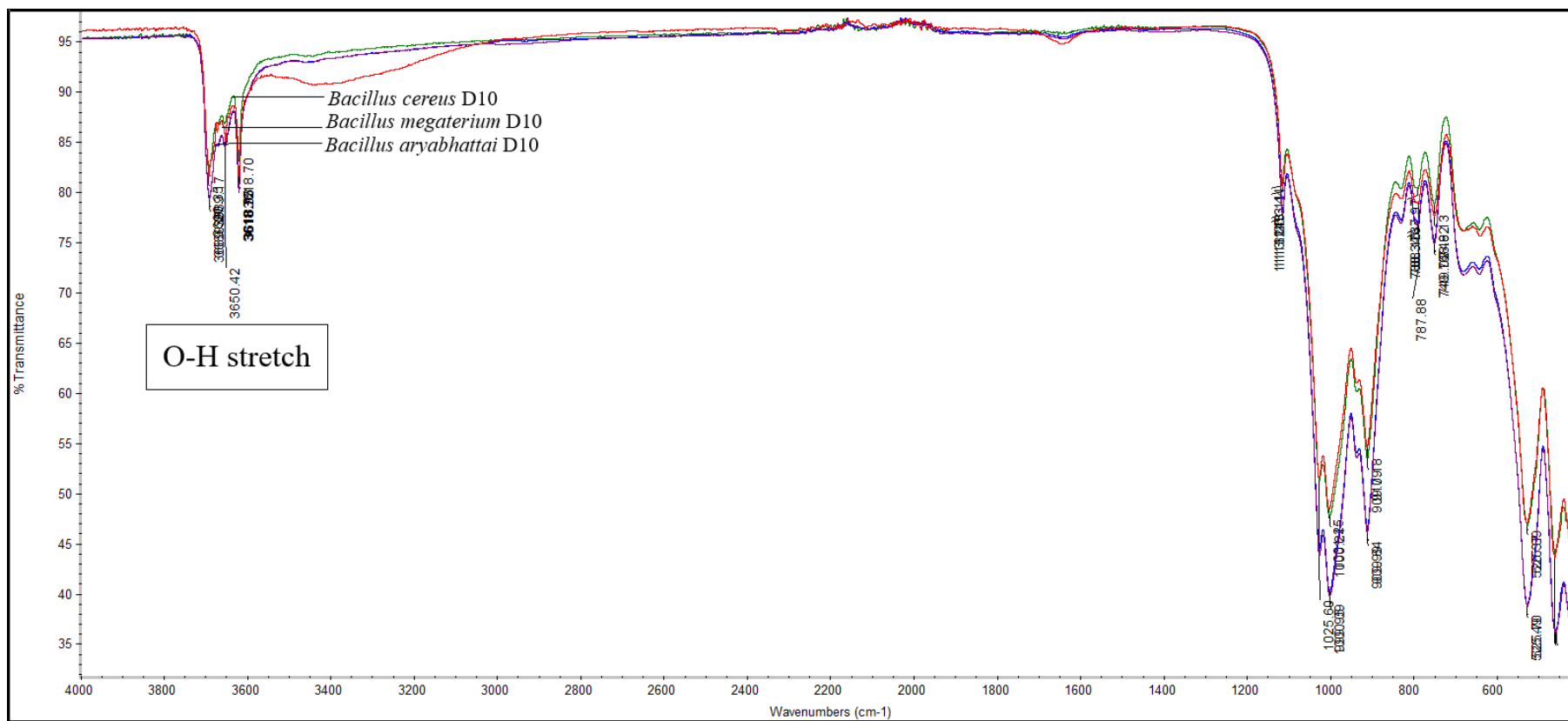
Figure 4.4(d): Comparison of FTIR for kaolin after treated with *B. cereus, B. aryabhattai* and *B. megaterium*

4.3   Acid Production of *Bacillus* sp. in Bioleaching

It is well known that glucose solution (10 g/L) acts as an ideal nutrient source for bacterial growth. *Bacillus* sp. obtains energy through cellular respiration, where glucose molecules are broken down into carbon dioxide and water to produce adenosine triphosphates (ATP) (Bonora et al., 2012). This means sufficiency of nutrient source is one of factors in optimising bioleaching efficiency (Guo et al., 2010). Based on the study of Guo et al. (2010), addition of $(NH_4)_2SO_4$ in bioleaching solution achieved iron dissolution of 3.4 mg Fe^{2+} per g of kaolin after 7 day incubations, slightly higher compared to that with only addition of carbon source, which achieved iron dissolution of 3.2 mg Fe^{2+} per g of kaolin. They concluded that addition of suitable nitrogen source, $(NH_4)_2SO_4$ able to accelerate bioleaching rate maybe because of nitrogen and sulfur is an essential element for bacterial activity (Štyriaková et al., 2007). However, addition of nitrogen source will incur extra cost at scale-up while the maximum iron dissolution is only slightly improved. Hence, the addition of nitrogen source in bioleaching treatment is not applied in this experiment.

Figure 4.5 shows the concentration of glucose medium which is measured at two days intervals for a 10-day period. All samples showed a progressive linear decrease in glucose concentration during the 10-day bioleaching period. Kaolin treated with *B. cereus* and *B. aryabhattai* showed the similar amounts of glucose consumption which is approximately 1.3 g/L. The glucose concentration of kaolin treated with *B. cereus* and *B. aryabhattai* dropped from 9.5 g/L on day 0 to 8.2 g/L on day 10 and 9.6 g/L on day 0 to 8.3

g/L on day 10 respectively. For kaolin treated with *B. megaterium*, glucose concentration decreased from 9.5 g/L on day 0 to 8.4 g/L on day 10 with approximately 1.1 g/L of glucose consumed. Across all samples, it was observed that the glucose concentration at day 10 still remained above 8.0 g/L indicating that there was still sufficient nutrient to sustain bacterial growth throughout the bioleaching period. The study of Reischke et al. (2015) showed adding at least 50 µg of glucose concentration to per gram of soil able to stimulate cellular respiration. The trend of glucose concentration in abiotic control decreased steadily from 9.6 g/L at day 0 to 9.0 g/L at day 10. The slight decrease in concentration of glucose solution in abiotic control may have been possibly caused by the oxidation of small amount of glucose molecules during the bioleaching period though more experiments will have to be conducted to validate this. What is certain is that the decrease of glucose levels in the abiotic sample remains minute compared to the ones treated with bacteria. This stark difference infers that bacteria is consuming the glucose, causing the drop in glucose levels for all samples treated with the three species respectively.
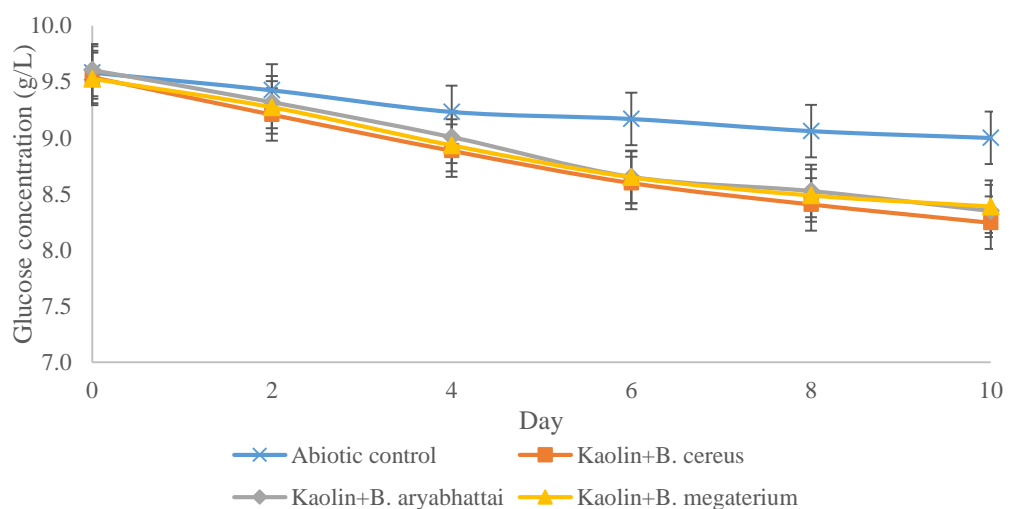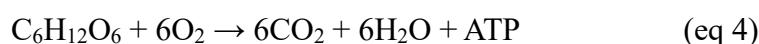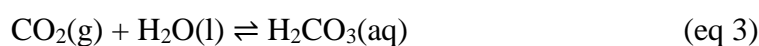

Figure 4.5: Glucose concentration in kaolin bioleaching with and without bacteria. Decrease of glucose concentration in bacteria-treated samples caused by the cellular respiration in *Bacillus* sp.

(Vertical bars shown in line graph represent the pooled standard deviation.)

Bacillus sp. obtained energy through cellular respiration, where glucose molecules are broken down to produce energy materials through glycolysis (Bonora et al., 2012). In kaolin bioleaching, glucose solution acts as an ideal nutrient source for the bacterial growth due to its existence in monosaccharide form. This form is characterised to be directly oxidised into the pyruvate molecules (Guo et al., 2010). Then the pyruvate molecules degraded into CO_2 and H_2O to produce ATP. CO_2 produced was dissolved in the medium and formed carbonic acid, H_2CO_3 (eq 3) (Mitchell et al., 2010). Under aerobic conditions, a total of 38 ATPs were produced, which were required for the bacterial growth (eq 4).

$$CO_2(g) + H_2O(l) \rightleftharpoons H_2CO_3(aq) \qquad\qquad (eq\ 3)$$

$$C_6H_{12}O_6 + 6O_2 \rightarrow 6CO_2 + 6H_2O + ATP \qquad\qquad (eq\ 4)$$

In this study, the glucose concentration still remained at 8.0 g/L and above in all the samples after the bioleaching (Figure 4.5). This clarified that there is sufficient nutrient source for bacterial growth since the largest consumption of glucose in these experiments were recorded at 1.3 g/L out of a total of 10 g/L of glucose concentration. Based on the study of effect of carbon source in kaolin bioleaching, Guo et al. (2010) indicated that monosaccharide is the most efficient followed by disaccharide and polysaccharide in the first four day. This is because disaccharide need to undergo hydrolysis to form either glucose or fructose whereas polysaccharide hydrolysed into dextrin followed by maltose, then only to fructose which can be taken by the bacterial cells (Elliott, 2004). However, the leaching efficiency of all samples reached the same level

45

after 10 days bioleaching (Figure 4.1) probably due to the decrease of carbon source concentration in the medium. Taken together, sufficiency of nutrient source is one of factors in optimising bioleaching efficiency whereas insufficient of nutrient source may be detrimental to the bacterial growth.

Besides glucose concentration, the pH value of glucose medium was also monitored at two days intervals during the bioleaching period. Figure 4.6 shows the changes of pH value of glucose medium with and without bacteria during bioleaching process. For abiotic control, the medium pH from day 0 to day 2 dropped slightly from 4.3 to 3.9. Then, it maintained at value of 3.9 until day 8 and decreased to 3.8 at day 10. In bioleaching, kaolin treated with *Bacillus* cereus showed a significant drop in medium pH value from 4.5 at day 0 to 2.9 at day 2 and showed a steady decreasing trend to 2.5 at day 10. Kaolin treated with *B. aryabhattai* and *B. megaterium* had the same initial pH value in medium which was 4.6 at day 0. For kaolin treated with *B. aryabhattai*, the pH value decreased steeply to 2.9 at day 2 and continued to decrease steadily until 2.5 at day 10. Similar results were observed in kaolin treated with *B. megaterium*, the pH value of the medium showed a sharp decline to 2.8 at day 2 and decreased slowly to 2.5 at day 10. Interestingly, pH values recorded for all three of the samples are similar so the trends showed in the graph overlapped with each other. This infers that while the presence of *Bacillus* is associated with notable drops in pH values, the trend of the decrement appears similar regardless of the *Bacillus* species employed.
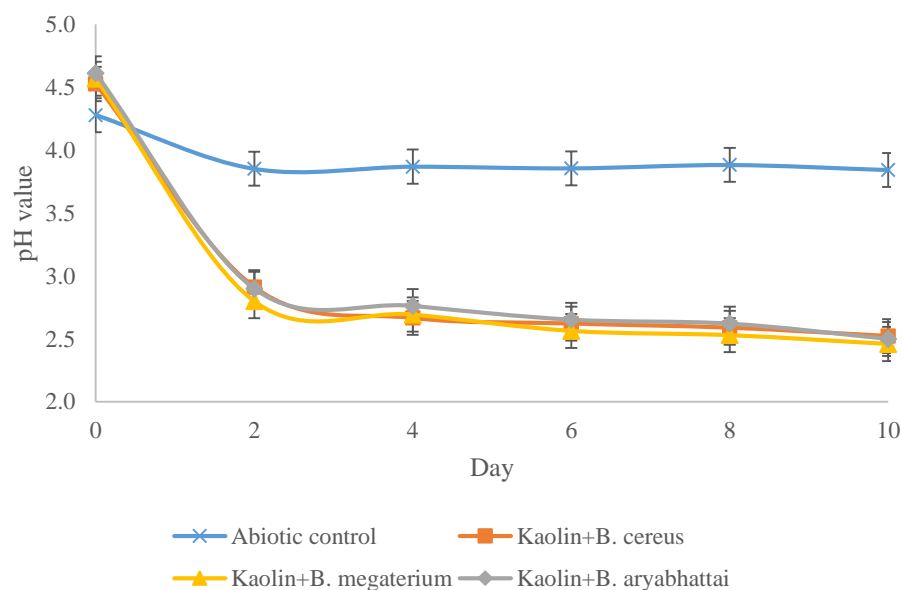
Figure 4.6: pH value in kaolin bioleaching with and without bacteria. The presence of *Bacillus* is associated with notable drops in pH values.
(Vertical bars shown in line graph represent the pooled standard deviation.)

The presence of organic acids, which are malic, acetic, formic, succinic, and lactic acid in bioleached samples were indicated by using Ion Chromatography and the results is shown in Table 4.3. Before the bioleaching process, no acid was detected in all of the samples. After the samples treated for 10 days, there was still no acid detected in abiotic control. However, malic acid and acetic acid with 15.3 ppm and 11.0 ppm respectively were detected in kaolin treated with *B. cereus*. For the sample treated with *B. aryabhattai*, there were five types of acids produced where lactic acid was the highest in concentration (170.0 ppm) followed by 53.3 ppm of formic acid, 17.0 ppm of malic acid, 7.77 ppm of acetic acid and 2.21 ppm of succinic acid. Similar with *B. aryabhattai*, *B. megaterium* also produced the most lactic acid with 126.4 ppm followed by 21.6 ppm of malic acid and 6.9 ppm of acetic acid during the bioleaching process.

47

Table 4.3: Acids produced by *Bacillus* sp. during bioleaching

Samples	Acids	Concentration (ppm)
Abiotic control	-	-
Kaolin treated with *B. cereus*	Malic acid	15.3 ± 0.44
	Acetic acid	11.0 ± 0.14
Kaolin treated with *B. aryabhattai*	Malic acid	17.0 ± 0.17
	Acetic acid	7.77 ± 0.02
	Formic acid	53.3 ± 0.01
	Succinic acid	2.21 ± 0.13
	Lactic acid	170.0 ± 0.03
Kaolin treated with *B. megaterium*	Malic acid	21.6 ± 0.26
	Acetic acid	6.9 ± 0.02
	Lactic acid	126.4 ± 0.04

The detected acids proved that *Bacillus* sp. produced organic acids as metabolites during the cell growth. In Štyriaková et al. (1999), acetic, butyric, pyruvic, lactic, and formic acid determined as main metabolites produced by *Bacillus* sp. Additionally, Saeid et al. (2018) indicated that *Bacillus* sp. generated lactate, acetate, succinate, gluconate, and propionate during the growth. These studies have indicated the types of organic acids produced during cell growth but the concentration of these acids has not determined. Besides, it is speculated that the organic acids produced by the bacteria leached the Fe(III) sites on kaolin surface and reduced Fe(III) to Fe(II). Therefore, organic acids produced by bacterial cells play a key role to reduce Fe(III) from kaolin.

In this study, organic acids produced by *B. cereus* were malate and acetate. For *B. aryabhattai*, the presence of malate, acetate, succinate, formate and lactate were detected in the sample. Other than that, malate, acetate and

lactate were produced by the *B. megaterium* during the cells growth. The production of organic acids was attributed to the leaching of Fe(III) and subsequent reduction to produce soluble Fe(II) (Lee et al., 2007). Overall, the production of organic acids by bacteria in these experiments are speculated to help leached the Fe(III) sites on the kaolin surface and improve the kaolin quality, converting the Fe(III) to Fe(II) in solution. This is further supported by o-phenanthroline results which proves increase in Fe(II) concentrations in samples treated with bacteria (Figure 4.1), glucose measurements which proves the depletion of glucose in samples treated with bacteria (Figure 4.5) and pH measurements which shows a progressively increasing acidic content of the bioleaching solution during 10-day period (Figure 4.6).

4.4   Surface Properties of Kaolin and Bacterial Cells

The zeta potential of each sample was measured at five-day intervals to study the surface properties in microbe-minerals surface interaction. Based on the results in Figure 4.7, kaolin treated with *B. cereus* showed similar trend with abiotic control, which the zeta potential decreased from day 0 to day 5 and increased again at day 10. For the abiotic control, the zeta potential was decreased from -0.87 mV at day 0 to -1.06 mV at day 5 before increased to -0.52 mV at day 10 within the close pH range of 4.3 to 3.8. The graph of abiotic control did not intercept the x-axis so no isoelectric point (IEP) was observed. IEP is the point of pH value at which the medium having overall charge of zero (Novák and Havlíček, 2016). This means that all the negative and positive charged ions in the medium is at equilibrium at this point. IEP also signifies a

49

point of charge reversal in the particles suspended in solution, from predominantly positive to predominantly negative and vice versa. The zeta potential value of abiotic control remained negatively charged during 10-day bioleaching. This infers that H^+ was not produced and the negative charge in the medium was probably from the charges of the raw kaolin.
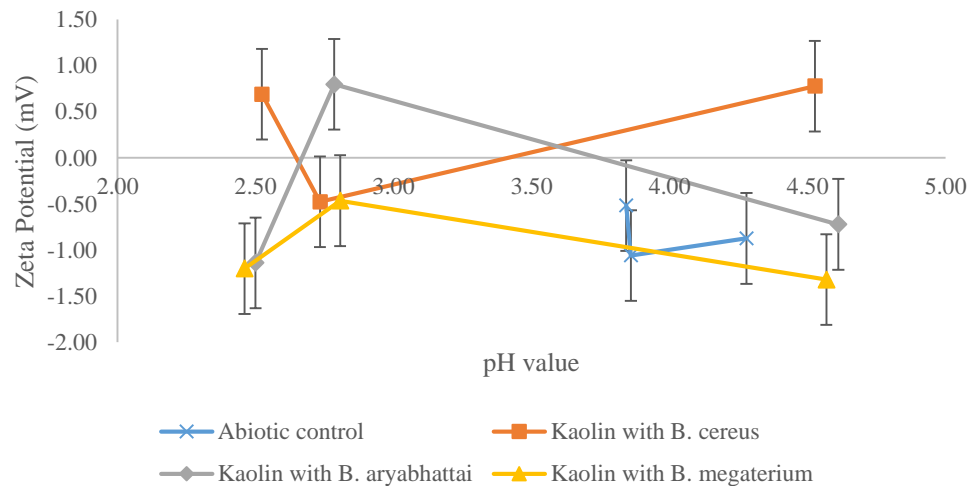

Figure 4.7: Zeta potential in interaction of kaolin with bacterial cells. The interaction of bacterial cells with kaolin surface altered the charge values of the solution which varies with pH value and bioleaching duration.
(Vertical bars shown in line graph represent the pooled standard deviation.)

For kaolin treated with *B. cereus*, zeta potential value started at 0.78 mV and it decreased linearly to -0.48 mV at day 5 and increased sharply back to 0.69 mV at day 10. This sample showed two isoelectric points (IEP) which are around pH of 3.40 and 2.60. In contrast, the zeta potential value of kaolin treated with *B. aryabhattai* and *B. megaterium* having the opposite trend with *B. cereus*, which increased from day 0 to day 5 then decreased at day 10. For the kaolin treated with *B. aryabhattai*, the zeta potential was increased from -0.72 mV at day 0 to 0.80 mV at day 5 then had a sudden drop to -1.14 mV at day 10. Besides, the zeta potential of kaolin treated with *B. megaterium* increased continuously

from -1.32 mV at day 0 to -0.46 mV at day 5 and decreased gradually to -1.20 mV at the last day. The zeta potential value measured in all samples is significantly different mostly due to the different types and concentration of acids produced by *Bacillus* sp. (Table 4.3). Kaolin treated with *B. aryabhattai* showed two IEP, first was around pH 3.80 and second was around pH 2.60. Although kaolin treated with *B. megaterium* had the similar pattern with *B. aryabhattai*, it did not show any interception at x-axis and thus no IEP was observed.

4.5   Bioleaching Efficiency of Other Studies

Table 4.4 showed the recent studies about bioleaching of kaolin using *Bacillus* species, *Aspergillus* species, *Shewanella* species and others. Based on the findings, *S. aureus* in the study of Jing et al. (2021) removed 76.2% of total ferric(III) oxide contaminant from kaolin after bioleached for 14 days. In the aspect of brightness index, *A. niger* (Musiał et al., 2011) and *Shewanella* sp. (Zegeye et al., 2013) showed similar performance, which the brightness index of kaolin increased from 74% to 79.2% and 74% to 79% respectively. Among the studies using *Bacillus* sp. listed in Table 4.4, the highest efficiency of Fe removal was 53.9% by Yap et al. (2020) after 5 days incubation followed by 53% by Štyriaková and Štyriak (2000) after 3 months bioleaching. Based on the EDS results in this study, kaolin treated with *B. cereus* showed bioleaching efficiency of 43.86% which is in common range compared with other studies, however, the bioleaching efficiency of kaolin treated with *B. aryabhattai* (13.57%) and *B. megaterium* (8.43%) is very lower than the usual range (more than 30%). The

EDS results may not depict the complete story as they are based on local concentrations measured by the SEM (Fe content of various sites on natural kaolin is expected to vary). The phenanthroline results paint a more accurate picture of Fe reduction taking place in the experiments and yield more consistent results (as shown in Figure 4.1). Direct comparison of phenanthroline results with Yap et al. (2020) show that they are in comparative ranges (1.43 mg/L vs 2.26 mg/L of maximum Fe(II) dissolution).

Table 4.4: Kaolin bioleaching efficiency in recent studies. (Adapted from Yong et al. (2022))

Microorganisms	Experimental setup	Bioleaching efficiency	Reference
Mixture of two *Bacillus cereus* strains	10 g of kaolin in 100 mL of modified Bromfield medium with 10^{10} cells/mL of bacterial culture. - Incubated at 28°C for 1 to 3 months under anaerobic conditions.	43% amorphous form Fe and approximately 15% of Fe attached on mica were removed after 1 month of bioleaching. - Removal of 53% bound Fe from kaolin after bioleaching time prolonged to 3 months.	(Štyriaková and Štyriak, 2000)
Bacillus cereus	10 g of kaolin in 100 mL of modified Bromfield medium with 10^{10} cells/mL of bacterial culture. - Incubated at 30°C for 3 months. - pH of samples maintained in range of 6-7.	Extraction of 49% iron atoms from the octahedral position in mica caused by bacterial activity.	(Štyriaková et al., 2003c)
Mixed culture of *Bacillus cereus, Bacillus sphaerius and Bacillus mycoides*	10 g of kaolin in 100 mL of medium with 1 g of carbon source and 5 mL of mixed culture broth. - Incubated at 30°C for 10 days.	- More than 50% of iron impurities was removed with whiteness index increased from 61% to 82% at 5% of food-sugar. - Addition of $(NH_4)_2SO_4$ accelerated the removal efficiency.	(Guo et al., 2010)
Aspergillus niger XP	A quantity of kaolin in 600 mL oxalic acid enriched medium (pH 3.0) at 100 rpm.	Brightness index of kaolin increased from 74% to 79.2%.	(Musiał et al., 2011)
Shewanella species (*S. alga* BrY*, S. oneidensis* MR-1*, S. putrefaciens* CN32,	10 or 20 g of kaolin in medium containing sodium methanoate, NaCl, AQDS and $3.0 \pm 1 \times 10^6$ to $1.05 \pm$	*S. putrefaciens* CIP8040 showed highest efficiency.	(Zegeye et al., 2013)

and S. putrefaciens CIP 8040)	0.35×10^7 CFU/mL of bacterial culture. • Incubated at 20 or 30°C in dark at 320 rpm for 5 days.	• ISO brightness increased from 74% to 79% and whiteness index from 54% to 66%.	
Aspergillus niger (*A. niger* NCIM 548, isolates strains from pistachio shell)	• 5 g of kaolin in 100 mL culture medium with 107 spores/cm^3 of cells. • Incubated at 30°C and 25°C with 160 rom for 14 to 28 days.	• *A. niger* isolated from pistachio skin removed 52% iron after 14 days, 47.7% after 28 days at 25°C. • Iron removal decreased to 33.8% after 28 days at 30°C.	(Hajihoseini and Fakharpour, 2019)
Bacillus cereus (*B. cereus* UKMTAR-4, *B. cereus* procured commercially)	• 10 g of kaolin in 80 mL glucose solution. • Incubated at 30°C with 250 rpm for 5 to 10 days.	• Fe removal by indigenous *B. cereus* strain UKMTAR-4 (53.9 %) and *B. cereus* procured commercially (33.9%). • Maximum Fe(II) dissolution increased from 1.19 to 2.26 mg/L when bacteria concentration increased from 3×10^8 CFU to 9×10^8 CFU.	(Yap et al., 2020)
Bacillus cereus UKMTAR-4, *Staphylococcus aureus* NCTC 6571, *Burkholderia thailandensis* MSMB43, *Escherichia coli* K-12, *Pseudomonas aeruginosa* DWW3	• 1 g of kaolin powder in 50 mL of nitrogen-rich medium. • Incubated at room temperature with 160 rpm for 14 days.	• Fe removal from total ferric(III) oxide contaminant by *S. aureus* (76.2%), *B. cereus* (38.7%) and *B. thailandensis* 31.4%. • Ferrous levels from cultures using *E. coli* or *P. aeruginosa* have no observable changes.	(Jing et al., 2021)

4.6   Fe Reduction Mechanism in Kaolin Bioleaching by *Bacillus* sp.

In glucose medium, *Bacillus* sp. obtained energy for cell growth through cellular respiration by breaking down glucose molecules into water and carbon dioxide to produce ATPs (Figure 4.8(a)). Carbon source in monosaccharides form such as glucose is known as the ideal nutrient source for bacterial growth as it is able to be degraded directly into pyruvate during glycolysis. Consequently, the glucose concentration of medium in samples with *Bacillus* sp. will decreased over times as the glucose molecules consumed by the bacterial cells.

The bioleaching process is speculated to have initiated with the attachment of bacterial cells onto kaolin surface through secretion of EPS, which majorly consisted of polysaccharides as well as proteins, nucleic acids and lipids to form complex combination of biopolymers (Flemming and Wingender, 2010). *Bacillus* sp. produced EPS to construct the intercellular space of microbial accumulated and this forms the biofilm matrix, which is important for the growth and survival of microorganisms (van Hullebusch et al., 2003; Vu et al., 2009). Kaolin surface which having negative charge attracted cations while the remaining positive charge of the cations attracted anions to form double diffuse layer. This prevents the attachment of bacterial cells on kaolin surface due to the repulsion force. However the production of EPS able to overcame the repulsion forces and bound to the Fe(III) site on kaolin surface with OH and/or COOH of the polysaccharides parts of EPS through hydrogen bonding (Figure 4.8(b)). *Bacillus* sp. attached on the kaolin surface through hydrogen bonding between the positive site of Fe(III) with OH (of the polysaccharides parts) and/or the

COOH present in polysaccharides and bacterial peptides (Selim and Rostom, 2018). This was supported by the FTIR results of all bacteria-treated samples where a band was observed at 3675 cm^{-1} which indicated the presence of O-H bonds.

During cell growth, *Bacillus* sp. produced organic acids as by-products of metabolism process. In this study, the organic acids produced by *B. cereus* were malate and acetate. For *B. aryabhattai*, the presence of malate, acetate, succinate, formate and lactate were indicated. Malate, acetate and lactate were made by *B. megaterium* during cell growth. The organic acids generated decreased the pH value of the medium. Besides, the production of organic acids by *Bacillus* sp. were responsible in reducing Fe(III) on kaolin to soluble Fe(II) (Figure 4.8(c)). EDS results showed that *Bacillus* sp. able to selectively reduced Fe(III) from kaolin without affecting much on chemical composition of other elements such Al, Si, K and O.

The production of organic acids definitely affected the charges in the medium due to the dissociation of H$^+$ ions. In the sample with *B. cereus*, the charge values of the sample decreased from positive value at day 0 to negative value at day 5 then increased again to positive value at day 10. For *B. aryabhattai* and *B. megaterium*, the zeta potential value increased from day 0 to day 5 but decreased at day 10. This analysis indicated that the interaction of bacterial cells with kaolin surface altered the charge values of the solution which varies with pH value and bioleaching duration.
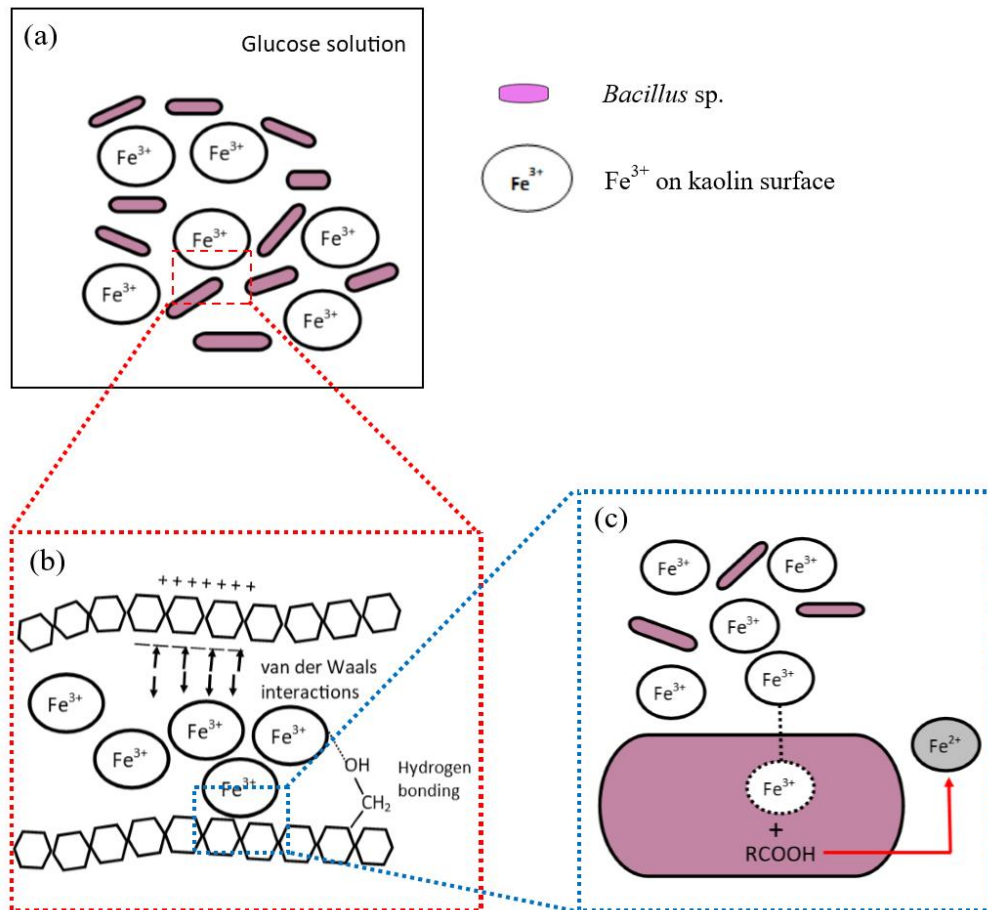
Figure 4.8: Fe reduction mechanism in kaolin bioleaching by *Bacillus* sp. (a) *Bacillus* sp. break down glucose molecules through cellular respiration to produce energy materials. (b) During attachment of bacterial cells on kaolin surface, positive Fe(III) sites on kaolin surface binds with the OH (polysaccharide portion) of EPS through hydrogen bonding. (c) During the cell growth, organic acids made by *Bacillus* sp. in metabolism process reduced Fe(III) to soluble Fe(II).

Furthermore, the bacterial activity in Fe(III) reduction damaged the edges of kaolin particles to be sharper. However, there was no formation of secondary minerals and no significant changes in structural modification was observed. Overall, *Bacillus* sp. is shown to be able to reduce Fe(III) from kaolin efficiently under optimised conditions. Even though some previous studies indicated the presence of organic acids during the bacterial growth, the concentrations of those acids have not been previously measured. Besides, there

is no mechanism of attachment of bacterial cell on kaolin surface related to production of acids and surface properties is proposed in previous study. In this study, a novel model is proposed involving the attachment of bacterial cell on kaolin surface where positive Fe(III) site binds with OH (polysaccharide portion) of EPS through hydrogen bonding as well as making of organic acids by bacterial cell to reduce Fe(III) in kaolin to soluble Fe(II) in kaolin bioleaching by *Bacillus* species. The model elucidates how the bacterial cells interact and behave in bioleaching conditions. The knowledge can be employed to remove Fe impurities sustainably from kaolin.

CHAPTER 5

CONCLUSION

In this work, the ability and bioleaching efficiency of Fe(III) reduction from kaolin by *B. cereus*, *B. aryabhattai* and *B. megaterium* has been determined using 1,10-phenanthroline assay. EDS analysis showed *Bacillus* sp. able to reduce Fe(III) from kaolin without affecting the chemical composition of other elements. Glucose concentration in the medium was shown to decrease progressively during bioleaching, most probably due to the cellular respiration of bacterial cell. In the experiments, kaolin treated with *Bacillus* sp. consumed 1.1-1.3 g/L of glucose while abiotic control only consumed 0.6 g/L of glucose. This indicated *Bacillus* sp. degraded glucose molecules to produce energy materials through cellular respiration. During the cell growth, *Bacillus* sp. produced organic acids as the by-products of metabolism. The organic acids produced by *B. cereus* were malate and acetate. For *B. aryabhattai*, the presence of malate, acetate, succinate, formate and lactate were detected. Besides, malate, acetate and lactate were generated by *B. megaterium* during the cell growth. The acids produced were responsible in reducing Fe(III) to soluble Fe(II). The presence of the organic acids was also supported by the decrease of pH value in medium during bioleaching process. The organic acids produced most probably reduced Fe(III) to Fe(II). In addition, SEM images showed leaching process by bacterial cells damaged the edges of the kaolin particles and appears sharper. While the comparison of abiotic control with raw kaolin showed no significant

difference, this indicated that the damaged edges observed in bacterial-treated samples was caused by the bacterial activities. However, XRD analysis for treated kaolin showed similar patterns with untreated kaolin indicated that there was no formation of secondary mineral phases and no structural modification in kaolinite was observed after the leaching process. Furthermore, based on FTIR analysis it was speculated that bacterial cells attached on kaolin surface through hydrogen bonding. A band that observed at 3675 cm^{-1} in the FTIR test suggested that *Bacillus* sp. attached on the kaolin surfaces through the positive site of Fe(III) with OH (of the polysaccharides parts) of the EPS. The interaction of bacterial cells with kaolin surface altered the zeta potential of the solution, the charge varies with pH value and bioleaching duration. Based on all these findings, a model of Fe reduction mechanism of kaolin by *Bacillus* sp. was proposed based on the results of this work. The proposed mechanism covered *Bacillus* sp. breaking down glucose molecules through cellular respiration to produce energy materials, attachment of bacterial cells on kaolin surface where Fe(III) sites on kaolin surface binds with the OH (polysaccharide portion) of EPS through hydrogen bonding and organic acids production by *Bacillus* sp. in metabolism process to reduce Fe(III) in kaolin to soluble Fe(II) in solution. Future work may include bacteria growth study in order to determine details and intricacies of bacteria growth during bioleaching such as the growth phase (set, early-log, middle-log, late-log, etc.) and effect of kaolin on bacteria growth during bioleaching. Ion chromatography analysis could also be conducted at much shorter intervals such as one or two-day intervals in order to analyze the evolution of organic acid production of the species during the bioleaching period. Furthermore, gene expression analysis can be performed using real-time

quantitative reverse transcription PCR to identify the genes that are responsible for producing organic acids involved in bioleaching. Identification of the genes responsible pave the way for more efficient optimization of the bioleaching process, because the specific genes can be modified for higher bioleaching efficiencies or bioleaching conditions can be optimized to enhance the expression of these genes. Besides, the usage of time-of-flight secondary ion mass spectrometry (ToF-SIMS) and cryogenic scanning transmission electron microscopy combined with electron-energy-loss spectroscopy (cryo-STEM-EELS) may enable examination of bacteria-kaolin interaction at atomic or molecular level. Such an analysis merits consideration because ToF-SIMS is useful in obtaining isotopic, elemental and molecular information from the kaolin surface while cryo-STEM-EELS allows the structural and chemical mapping of bacterial-mineral interaction interfaces at nanometer scale.

REFERENCES

Abdel-Khalek, N.A., Selim, K.A., Abdallah, S.S., Yassin, K.E., 2013. Bioflotation of low grade Egyptian Iron ore using Brevundimonas diminuta bacteria: Phosphorus removal. Elixir Bio Technol. 63, 18666–18670.

Adams, J.M., Hopper, J.J., Gil, A., 2016. Clays. Ref. Modul. Mater. Sci. Mater. Eng. 1–8. https://doi.org/10.1016/B978-0-12-803581-8.02327-4

Arslan, V., Bayat, O., 2009. Removal of Fe from kaolin by chemical leaching and bioleaching. Clays Clay Miner. 57, 787–794. https://doi.org/10.1346/CCMN.2009.05706011

Asghari, I., Mousavi, S.M., Amiri, F., Tavassoli, S., 2013. Bioleaching of spent refinery catalysts : A review. J. Ind. Eng. Chem. 19, 1069–1081. https://doi.org/10.1016/j.jiec.2012.12.005

Bajpai, P., 2018. Papermaking chemistry, in: Biermann's Handbook of Pulp and Paper. pp. 207–236. https://doi.org/10.1016/B978-0-12-814238-7.00010-6

Belyadi, H., Fathi, E., Belyadi, F., 2019. Hydraulic fracturing chemical selection and design. Hydraul. Fract. Unconv. Reserv. 107–120. https://doi.org/10.1016/b978-0-12-817665-8.00008-4

Bleam, W.F., 2012. Redox Chemistry, in: Soil and Environmental Chemistry. pp. 321–370. https://doi.org/10.1016/B978-0-12-415797-2.00008-X

Bonora, M., Patergnani, S., Rimessi, A., Marchi, E. De, Suski, J.M., Bononi, A., Giorgi, C., Marchi, S., Missiroli, S., Poletti, F., 2012. ATP synthesis and storage. Purinergic Signal. 8, 343–357. https://doi.org/10.1007/s11302-012-9305-8

Cameselle, C., Ricart, M.T., Núñez, M.J., Lema, J.M., 2003. Iron removal from kaolin. Comparison between "in situ" and "two-stage" bioleaching processes. Hydrometallurgy 68, 97–105. https://doi.org/10.1016/S0304-386X(02)00196-2

Cao, Y., Wei, X., Cai, P., Huang, Q., Rong, X., Liang, W., 2011. Preferential adsorption of extracellular polymeric substances from bacteria on clay minerals and iron oxide. Colloids Surfaces B Biointerfaces 83, 122–127. https://doi.org/10.1016/j.colsurfb.2010.11.018

Chandraprabha, M.N., Natarajan, K.A., 2010. Microbially induced mineral beneficiation. Miner. Process. Extr. Metall. Rev. 31, 1–29. https://doi.org/10.1080/08827500903404682

Comensoli, L., Maillard, J., Albini, M., Sandoz, F., Junier, P., Joseph, E., 2017. Use of bacteria to stabilize archaeological iron. Appl. Environ. Microbiol.

89. https://doi.org/10.1128/AEM.03478-16

Conley, R.F., Lloyd, M.K., 1970. Improvement of iron leaching in clays. Ind. Eng. Chem. Process Des. Dev. 9, 595–601.

Du, H., Yu, G., Sun, F., Usman, M., Goodman, B.A., Ran, W., Shen, Q., 2019. Iron minerals inhibit the growth of *Pseudomonas brassicacearum* J12 via a free-radical mechanism: implications for soil carbon storage. Biogeosciences 16, 1433–1445.

Ebrahiminezhad, A., Manafi, Z., Berenjian, A., Kianpour, S., 2017. Iron-reducing bacteria and iron nanostructures. J. Adv. Med. Sci. Appl. Technol. 3, 9–15. https://doi.org/10.18869/nrip.jamsat.3.1.9

Elliott, D.C., 2004. Biomass , Chemicals from. Encycl. od Energy 1, 163–174.

Fakharpour, M., Hajihoseini, J., 2021. Optimal removal of iron impurities from kaolin by combination of *Aspergillus niger* & *Bacillus subtilis*. Int. J. Mater. Res. 112, 498–504. https://doi.org/Fakharpour, M., & Hajihoseini, J. (2021). Optimal removal of iron impurities from kaolin by combination of Aspergillus niger & Bacillus subtilis. International Journal of Materials Research, 112(6), 498–504. https://doi.org/10.1515/ijmr-2020-8048

Flemming, H.C., Wingender, J., 2010. The biofilm matrix. Nat. Rev. Microbiol. 8, 623–633. https://doi.org/10.1038/nrmicro2415

Galán, E., 2006. Genesis of clay minerals, in: Bergaya, F., Theng, B.K.G., Lagaly, G. (Eds.), Handbook of Clay Science. Elsevier Ltd., pp. 1129–1162. https://doi.org/10.1016/S1572-4352(05)01042-1

Ghashoghchi, R.A., Hosseini, M.R., Ahmadi, A., 2017. Effects of microbial cells and their associated extracellular polymeric substances on the bio-flocculation of kaolin and quartz. Appl. Clay Sci. 138, 81–88. https://doi.org/10.1016/j.clay.2017.01.002

Ghorbani, Y., Oliazadeh, M., Shahvedi, A., Roohi, R., Pirayehgar, A., 2007. Use of some isolated fungi in biological leaching of aluminum from low grade bauxite. African J. Biotechnol. 6, 1284–1288. https://doi.org/10.5897/AJB2007.000-2178

Gougazeh, M., 2018. Removal of iron and titanium contaminants from Jordanian Kaolins by using chemical leaching. J. Taibah Univ. Sci. 12, 247–254. https://doi.org/10.1080/16583655.2018.1465714

Guo, M.R., Lin, Y.M., Xu, X.P., Chen, Z.L., 2010. Bioleaching of iron from kaolin using Fe(III)-reducing bacteria with various carbon nitrogen sources. Appl. Clay Sci. 48, 379–383. https://doi.org/10.1016/j.clay.2010.01.010

Hajihoseini, J., Fakharpour, M., 2019. Effect of temperature on bioleaching of iron impurities from kaolin by *Aspergillus niger* fungal. J. Asian Ceram.

Soc. 1–8. https://doi.org/10.1080/21870764.2019.1571152

Herrera, L., Ruiz, P., Aguillon, J.C., Fehrmann, A., 1989. A new spectrophotometric method for the determination of ferrous iron in the presence of ferric iron. J. Chem. Technol. Biotechnol. 44, 171–181. https://doi.org/10.1002/jctb.280440302

Holešová, S., Samlíková, M., Pazdziora, E., Valášková, M., 2013. Antibacterial activity of organomontmorillonites and organovermiculites prepared using chlorhexidine diacetate. Appl. Clay Sci. 83–84, 17–23. https://doi.org/10.1016/j.clay.2013.07.013

Hori, K., Matsumoto, S., 2010. Bacterial adhesion: From mechanism to control. Biochem. Eng. J. 48, 424–434. https://doi.org/10.1016/j.bej.2009.11.014

Hosseini, M.R., Ahmadi, A., 2015. Biological beneficiation of kaolin: A review on iron removal. Appl. Clay Sci. 107, 238–245. https://doi.org/10.1016/j.clay.2015.01.012

Hosseini, M.R., Pazouki, M., Ranjbar, M., Habibian, M., 2007. Bioleaching of iron from highly contaminated kaolin clay by *Aspergillus niger*. Appl. Clay Sci. 37, 251–257. https://doi.org/10.1016/j.clay.2007.01.010

Ikogou, M., Ona-nguema, G., Juillot, F., Le, P., Brest, J., Menguy, N., Richeux, N., Guigner, J., No, V., Baptiste, B., Morin, G., 2017. Long-term sequestration of nickel in mackinawite formed by *Desulfovibrio capillatus* upon Fe(III)-citrate reduction in the presence of thiosulfate. Appl. Geochemistry 80, 143–154. https://doi.org/10.1016/j.apgeochem.2017.02.019

Jing, H., Liu, Z., Kuan, S.H., Chieng, S., Ho, C.L., 2021. Elucidation of gram-positive bacterial iron(III) reduction for kaolinite clay refinement. Molecules 26, 3084.

Jou, S.K., Nik Malek, N.A.N., 2016. Characterization and antibacterial activity of chlorhexidine loaded silver-kaolinite. Appl. Clay Sci. 127–128, 1–9. https://doi.org/10.1016/j.clay.2016.04.001

Kato, T., Toyooka, T., Ibuki, Y., Masuda, S., Watanabe, M., Totsuka, Y., 2017. Effect of physicochemical character differences on the genotoxic potency of kaolin. Genes Environ. 39, 1–10. https://doi.org/10.1186/s41021-017-0075-y

Kawanishi, M., Yoneda, R., Totsuka, Y., Yagi, T., 2020. Genotoxicity of micro- and nano-particles of kaolin in human primary dermal keratinocytes and fibroblasts. Genes Environ. 42, 1–7. https://doi.org/10.1186/s41021-020-00155-1

Khan, M.S.A., Altaf, M.M., Ahmad, I., 2017. Chemical nature of biofilm matrix and its significance, in: Biofilms in Plant and Soil Health. pp. 151–177.

https://doi.org/10.1002/9781119246329.ch9

Lee, E.Y., Cho, K.-S., Ryu, H.W., 2002. Microbial refinement of kaolin by iron-reducing bacteria. Appl. Clay Sci. 22, 47–53. https://doi.org/10.1016/S0169-1317(02)00111-4

Lee, S.O., Tran, T., Jung, B.H., Kim, S.J., Kim, M.J., 2007. Dissolution of iron oxide using oxalic acid. Hydrometallurgy 87, 91–99. https://doi.org/10.1016/j.hydromet.2007.02.005

Lempp, M., Lubrano, P., Bange, G., Link, H., 2020. Metabolism of non-growing bacteria. Biol. Chem. 401, 1479–1485. https://doi.org/10.1515/hsz-2020-0201

Liu, D., Wang, F., Dong, H., Wang, H., Zhao, L., Huang, L., Wu, L., 2016. Biological reduction of structural Fe(III) in smectites by a marine bacterium at 0.1 and 20 MPa. Chem. Geol. 438, 1–10. https://doi.org/10.1016/j.chemgeo.2016.05.020

Liu, G., Qiu, S., Liu, B., Pu, Y., Gao, Z., Wang, J., Jin, R., Zhou, J., 2017. Microbial reduction of Fe(III)-bearing clay minerals in the presence of humic acids. Sci. Rep. 7, 1–9. https://doi.org/10.1038/srep45354

Merino, C., Kuzyakov, Y., Godoy, K., Jofré, I., Nájera, F., Matus, F., 2020. Iron-reducing bacteria decompose lignin by electron transfer from soil organic matter. Sci. Total Environ. 761, 143194. https://doi.org/10.1016/j.scitotenv.2020.143194

Mitchell, M.J., Jensen, O.E., Cliffe, K.A., Maroto-Valer, M.M., 2010. A model of carbon dioxide dissolution and mineral carbonation kinetics. Proc. R. Soc. A Math. Phys. Eng. Sci. 466, 1265–1290. https://doi.org/10.1098/rspa.2009.0349

Moraes, J.D.D., Bertolino, S.R.A., Cuffini, S.L., Ducart, D.F., Bretzke, P.E., Leonardi, G.R., 2017. Clay minerals: Properties and applications to dermocosmetic products and perspectives of natural raw materials for therapeutic purposes—A review. Int. J. Pharm. 534, 213–219. https://doi.org/10.1016/j.ijpharm.2017.10.031

Mueller, K.T., Sanders, R.L., Washton, N.M., 2014. Clay minerals. eMagRes 3, 13–28. https://doi.org/10.1002/9780470034590.emrstm1332

Musiał, I., Cibis, E., Rymowicz, W., 2011. Designing a process of kaolin bleaching in an oxalic acid enriched medium by *Aspergillus niger* cultivated on biodiesel-derived waste composed of glycerol and fatty acids. Appl. Clay Sci. 52, 277–284. https://doi.org/10.1016/j.clay.2011.03.004

Natarajan, K.A., 2018. Microbially induced mineral beneficiation, Biotechnology of Metals. Elsevier Inc. https://doi.org/10.1016/b978-0-12-804022-5.00010-4

Neto, J.C. de M., Nascimento, N.R. do, Bello, R.H., Verçosa, L.A. de, Neto, J.E., 2022. Kaolinite review: Intercalation and production of polymer nanocomposites. Eng. Sci. 17, 28–44. https://doi.org/10.30919/es8d499

Notini, L., Byrne, J.M., Tomaszewski, E.J., Latta, D.E., Zhou, Z., Scherer, M.M., Kappler, A., 2019. Mineral defects enhance bioavailability of goethite toward microbial Fe(III) reduction. Environ. Sci. Technol. 53, 8883–8891. https://doi.org/10.1021/acs.est.9b03208

Novák, P., Havlíček, V., 2016. Protein extraction and precipitation, in: Proteomic Profiling and Analytical Chemistry: The Crossroads: Second Edition. pp. 52–62. https://doi.org/10.1016/B978-0-444-63688-1.00004-5

Pentráková, L., Su, K., Pentrák, M., Stucki, J.W., 2013. A review of microbial redox interactions with structural Fe in clay minerals. Clay Miner. 48, 543–560. https://doi.org/10.1180/claymin.2013.048.3.10

Perdrial, J.N., Warr, L.N., Perdrial, N., Lett, M.C., Elsass, F., 2009. Interaction between smectite and bacteria: Implications for bentonite as backfill material in the disposal of nuclear waste. Chem. Geol. 264, 281–294. https://doi.org/10.1016/j.chemgeo.2009.03.012

Poorni, S., Natarajan, K.A., 2014. Flocculation behaviour of hematite-kaolinite suspensions in presence of extracellular bacterial proteins and polysaccharides. Colloids Surfaces B Biointerfaces 114, 186–192. https://doi.org/10.1016/j.colsurfb.2013.09.049

Poorni, S., Natarajan, K.A., 2013. Microbially induced selective flocculation of hematite from kaolinite. Int. J. Miner. Process. 125, 92–100. https://doi.org/10.1016/j.minpro.2013.10.002

Qiu, H., Xu, H., Xu, Z., Xia, B., Peijnenburg, W.J.G.M., Cao, X., Du, H., Zhao, L., Qiu, R., He, E., 2020. The shuttling effects and associated mechanisms of different types of iron oxide nanoparticles for Cu(II) reduction by Geobacter sulfurreducens. J. Hazard. Mater. 393, 122390. https://doi.org/10.1016/j.jhazmat.2020.122390

Rawski, D.P., Bhuiyan, M., 2017. Pulp and paper: Nonfibrous components. Ref. Modul. Mater. Sci. Mater. Eng. 1–4. https://doi.org/10.1016/B978-0-12-803581-8.10289-9

Reischke, S., Kumar, M.G.K., Bååth, E., 2015. Threshold concentration of glucose for bacterial growth in soil. Soil Biol. Biochem. 80, 218–223. https://doi.org/10.1016/j.soilbio.2014.10.012

Saeid, A., Prochownik, E., Dobrowolska-Iwanek, J., 2018. Phosphorus solubilization by *Bacillus* species. Molecules 23, 1–18. https://doi.org/10.3390/molecules23112897

Selim, K.A., Rostom, M., 2018. Bioflocculation of (Iron oxide- Silica) system

using *Bacillus cereus* bacteria isolated from Egyptian iron ore surface. Egypt. J. Pet. 27, 235–240. https://doi.org/10.1016/j.ejpe.2017.07.002

Seredin, V. V, Andrianov, A. V, Gaynanov, S.K., Galkin, V.I., Andreyko, S.S., 2021. Formation of the kaolin structure treated by pressure. Perm J. Pet. Min. Eng. 21, 9–16. https://doi.org/10.15593/2712-8008/2021.1.2

Shelobolina, E.S., Vanpraagh, C.G., Lovley, D.R., 2003. Use of ferric and ferrous iron containing minerals for respiration by *Desulfitobacterium frappieri*. Geomicrobiol. J. 20, 143–156. https://doi.org/10.1080/01490450303884

Strasser, H., Burgstaller, W., Schinner, F., 1994. High-yield production of oxalic acid for metal leaching processes by *Aspergillus niger*. FEMS Microbiol. Lett. 119, 365–370. https://doi.org/10.1016/0378-1097(94)90441-3

Štyriaková, I.., Štyriak, I., Malachovsky, P., 2007. Nutrients Enhancing the Bacterial Iron Dissolution in the Processing of Feldspar Raw Materials. Ceram. − Silikáty 51, 202–209.

Štyriaková, I., Štyriak, I., 2000. Iron removal from kaolins by bacterial leaching. Ceram. - Silikáty 44, 135–141.

Štyriaková, I., Štyriak, I., Galko, I., Hradil, D., Bezdička, P., 2003a. The release of iron-bearing minerals and dissolution of feldspars by heterotrophic bacteria of *Bacillus* species. Ceram. - Silikaty 47, 20–26.

Štyriaková, I., Štyriak, I., Kraus, I., Hradil, D., Grygar, T., Bezdička, P., 2003b. Biodestruction and deferritization of quartz sands by Bacillus species. Miner. Eng. 16, 709–713. https://doi.org/10.1016/S0892-6875(03)00165-1

Štyriaková, I., Štyriak, I., Kušnierová, M., 1999. The release of sulphidic minerals from aluminosilicates by *Bacillus* strains, in: Process Metallurgy. pp. 587–596. https://doi.org/10.1016/S1572-4409(99)80060-1

Štyriaková, I., Štyriak, I., Nandakumar, M.P., Mattiasson, B., 2003c. Bacterial destruction of mica during bioleaching of kaolin and quartz sands by *Bacillus cereus*. World J. Microbiol. Biotechnol. 19, 583–590.

Telegdi, J., Shaban, A., Vastag, G., 2018. Biocorrosion-steel. Encycl. Interfacial Chem. Surf. Sci. Electrochem. 28–42. https://doi.org/10.1016/B978-0-12-409547-2.13591-7

Thirumalai, M., 2020. Effects of salt, vinegar and bleach in accelerating rusting of iron. Int. J. Innov. Res. Adv. Stud. 7, 20–26.

Thurlow, C., 2001. China clay from Cornwall and Devon — The modern China clay industry. Cornish Hillside Publication, St. Austell, Cornwall.

Tsuneda, S., Aikawa, H., Hayashi, H., Yuasa, A., Hirata, A., 2003. Extracellular

polymeric substances responsible for bacterial adhesion onto solid surface. FEMS Microbiol. Lett. 223, 287–292. https://doi.org/10.1016/S0378-1097(03)00399-9

Uddin, F., 2018. Montmorillonite: An introduction to properties and utilization, in: Current Topics in the Utilization of Clay in Industrial and Medical Applications. InTech, pp. 3–24. https://doi.org/10.5772/intechopen.77987

van Hullebusch, E.D., Zandvoort, M.H., Lens, P.N.L., 2003. Metal immobilisation by biofilms: Mechanisms and analytical tools. Rev. Environ. Sci. Bio/Technology 2, 9–33. https://doi.org/10.1023/B:RESB.0000022995.48330.55

Vardanyan, A., Vyrides, I., 2019. Acidophilic bioleaching at high dissolved organic compounds: Inhibition and strategies to counteract this. Miner. Eng. 143, 105943. https://doi.org/10.1016/j.mineng.2019.105943

Vu, B., Chen, M., Crawford, R.J., Ivanova, E.P., 2009. Bacterial extracellular polysaccharides involved in biofilm formation. Molecules 14, 2535–2554. https://doi.org/10.3390/molecules14072535

Warr, L.N., Perdrial, J.N., Lett, M.C., Heinrich-Salmeron, A., Khodja, M., 2009. Clay mineral-enhanced bioremediation of marine oil pollution. Appl. Clay Sci. 46, 337–345. https://doi.org/10.1016/j.clay.2009.09.012

Yap, H.J., Yong, S.N., Cheah, W.Q., Chieng, S., Kuan, S.H., 2020. Bioleaching of kaolin with *Bacillus cereus*: Effect of bacteria source and concentration on iron removal. J. Sustain. Sci. Manag. 15, 91–99. https://doi.org/10.46754/jssm.2020.06.009

Yong, S.N., 2019. Pengoptimuman unit pembentukan koloni *Bacillus cereus* dalam larut lesap besi daripada kaolin. Universiti Kebangsaan Malaysia.

Yong, S.N., Lim, S., Ho, C.L., Chieng, S., Kuan, S.H., 2022. Mechanisms of microbial-based iron reduction of clay minerals: Current understanding and latest developments. Appl. Clay Sci. 228, 106653. https://doi.org/10.1016/j.clay.2022.106653

Zegeye, A., Yahaya, S., Fialips, C.I., White, M.L., Gray, N.D., Manning, D.A.C., 2013. Refinement of industrial kaolin by microbial removal of iron-bearing impurities. Appl. Clay Sci. 86, 47–53. https://doi.org/10.1016/j.clay.2013.08.041

Zhao, H., Zhang, Y., Zhang, X., Qian, L., Sun, M., Yang, Y., Zhang, Y., Wang, J., Kim, H., Qiu, G., 2019. The dissolution and passivation mechanism of chalcopyrite in bioleaching: An overview. Miner. Eng. 136, 140–154. https://doi.org/10.1016/j.mineng.2019.03.014

APPENDIX A

Table below shows the sequencing results for the isolated colonies from kaolin. The results shows Colony 1, 2 and 4 are *Bacillus aryabhattai, Bacillus megaterium* and *Bacillus cereus* respectively. Three of these *Bacillus* sp. were tested in kaolin bioleaching. Colony 3, 5 and 6 are not included in study due to sequencing results unable to differentiate Colony 3 between *B. aryabhattai* or *B.* megaterium, the species of Colony 5 is still under study and lack of genomic information whereas Colony 6 is harmful and might causes severe infections in human body system.

Colony	Sequence	Sequence Number	Organisms Name	Identities (%)	Score (bits)	E value
1	CTGGGACTGAGACACGGCCCAGACTCCTACGGGAGGCAGCAGTAGGGAA TCTTCCGCAATGGACGAAAGTCTGACGGAGCAACGCCGCGTGAGTGATG AAGGCTTTCGGGTCGTAAAACTCTGTTGTTAGGGAAGAACAAGTACAAG AGTAACTGCTTGTACCTTGACGGTACCTAACCAGAAAGCCACGGCTAACT ACGTGCCAGCAGCCGCGGTAATACGTAGGTGGCAAGCGTTATCCGGAATT ATTGGGCGTAAAGCGCGCGCAGGCGGTTTCTTAAGTCTGATGTGGAAGCC CACGGCTCAACCGTGGAGGGTCATTGGAAACTGGGGAACTTGAGTGCAG AAGAGAAAAGCGGAATTCCACGTGTAGCGGTGAAATGCGTAGAGATGTG GAGGAACACCAGTGGCGAAGGCGGCTTTTTGGTCTGTAACTGACGCTGA GGCGCGAAAGCGTGGGGAGCAAACAGGATTAGATACCCTGGTAGTCCAC GCCGTAAACGATGAGTGCTAAGTGTTAGAGGGTTTCCGCCCTTTAGTGCT GCAGCTAACGCATTAAGCACTCCGCCTGGGGAGTACGGTCGCAAGACTG AAACTCAAAGGAATTGACGGGGGCCCGCACAAGCGGTGGAGCATGTGGT TTAATTCGAAGCAACGCGAAGAACCTTACCAGGTCTTGACATCCTCTGAC AACTCTAGAGATAGAGCGTTCCCCTTCGGGGG	KF150411.1	*Bacillus aryabhattai strain JN162*	100.00	1336	0.0
		ON891972.1	*Priestia aryabhattai strain NIOT_A*	100.00	1336	0.0
		MN181355.1	*Bacillus flexus strain T3-19*	99.86	1330	0.0
2	AATCTTCCGCAATGGACGAAAGTCTGACGGAGCAACGCCGCCTGAGTGAT GAAGGCTTTCGGGTCGTAAAACTCTGTTGTTAGGGAAGAACAAGTACGA GAGTAACTGCTCGTACCTTGACGGTACCTAACCAGAAAGCCACGGCTAAC TACGTGCCAGCAGCCGCGGTAATACGTAGGTGGCAAGCGTTATCCGGAAT TATTGGGCGTAAAGCGCGCGCAGGCGGTTTCTTAAGTCTGATGTGAAAGC CCACGGCTCAACCGTGGAGGGTCATTGGAAACTGGGGAACTTGAGTGCA GAAGAGAAAAGCGGAATTCCACGTGTAGCGGTGAAATGCGTAGAGATGT	MT453994.1	*Bacillus megaterium strain S1*	99.88	1568	0.0
		MK598810.1	*Bacillus megaterium strain 5A1-13*	99.88	1568	0.0
		MN994080.1	*Bacillus megaterium*	99.88	1568	0.0

	GGAGGAACACCAGTGGCGAAGGCGGCTTTTTGGTCTGTAACTGACGCTG AGGCGCGAAAGCGTGGGGAGCAAACAGGATTAGATACCCTGGTAGTCCA CGCCGTAAACGATGAGTGCTAAGTGTTAGAGGGTTTCCGCCCTTTAGTGC TGCAGCTAACGCATTAAGCACTCCGCCTGGGGAGTACGGTCGCAAGACTG AAACTCAAAGGAATTGACGGGGGCCCGCACAAGCGGTGGAGCATGTGGT TTAATTCGAAGCAACGCGAAGAACCTTACCAGGTCTTGACATCCTCTGAC AACTCTAGAGATAGAGCGTTCCCCTTCGGGGGACAGAGTGACAGGTGGT GCATGGTTGTCGTCAGCTCGTGTCGTGAGATGTTGGGTTAAGTCCCGCAA CGAGCGCAACCCTTGATCTTAGTTGCCAGCATTCAGTTGGGCACTCTAAG GTGACTGCCGGTGACAAACCGGAGGAAGGTGGGGATGACGTCAAATCAT CATGCCCCTT		*strain SBJR0904*			
3	TCCCCCGAAGGGGAACGCTCTATCTCTAGAGTTGTCAGAGGATGTCAAGA CCTGGTAAGGTTCTTCGCGTTGCTTCGAATTAAACCACATGCTCCACCGCT TGTGCGGGCCCCCGTCAATTCCTTTGAGTTTCAGTCTTGCGACCGTACTCC CCAGGCGGAGTGCTTAATGCGTTAGCTGCAGCACTAAAGGGCGGAAACC CTCTAACACTTAGCACTCATCGTTTACGGCGTGGACTACCAGGGTATCTAA TCCTGTTTGCTCCCCACGCTTTCGCGCCTCAGCGTCAGTTACAGACCAAA AAGCCGCCTTCGCCACTGGTGTTCCTCCACATCTCTACGCATTTCACCGCT ACACGTGGAATTCCGCTTTTCTCTTCTGCACTCAAGTTCCCCAGTTTCCAA TGACCCTCCACGGTTGAGCCGTGGGCTTTCACATCAGACTTAAGAAACCG CCTGCGCGCGCTTTACGCCCAATAATTCCGGATAACGCTTGCCACCTACGT ATTACCGCGGCTGCTGGCACGTAGTTAGCCGTGGCTTTCTGGTTAGGTACC GTCAAGGTACGAGCAGTTACTCCGTACTTGTTCTTCCCTAACAACAGAG TTTTACGACCCGAAAGCCTTCATCACTCACGCGGCGTTGCTCCGTCAGAC TTTCGTCCATTGCGGAAGATTCC	OP458197.1	*Priestia aryabhattai B8W22*	100.00	1254	0.0
		OP457078.1	*Priestia aryabhattai strain TCI-16*	100.00	1254	0.0
		OP410984.1	*Priestia megaterium strain Cons_Bm_SDBBA*	100.00	1254	0.0
4	CCGCAATGGACGAAAGTCTGACGGAGCAACGCCGCGTGAGTGATGAAGG CTTTCGGGTCGTAAAACTCTGTTGTTAGGGAAGAACAAGTGCTAGTTGAA TAAGCTGGCACCTTGACGGTACCTAACCAGAAAGCCACGGCTAACTACGT GCCAGCAGCCGCGGTAATACGTAGGTGGCAAGCGTTATCCGGAATTATTG GGCGTAAAGCGCGCGCAGGTGGTTTCTTAAGTCTGATGTGAAAGCCCACG GCTCAACCGTGGAGGGTCATTGGAAACTGGGAGACTTGAGTGCAGAAGA GGAAAGTGGAATTCCATGTGTAGCGGTGAAATGCGTAGAGATATGGAGGA ACACCAGTGGCGAAGGCGACTTTCTGGTCTGTAACTGACACTGAGGCGC GAAAGCGTGGGGAGCAAACAGGATTAGATACCCTGGTAGTCCACGCCGTA AACGATGAGTGCTAAGTGTTAGAGGGTTTCCGCCCTTTAGTGCTGAAGTT AACGCATTAAGCACTCCGCCTGGGGAGTACGGCCGCAAGGCTGAAACTC AAAGGAATTGACGGGGGCCCGCACAAGCGGTGGAGCATGTGGTTTAATTC GAAGCAACGCGAAGAACCTTACCAGGTCTTGACATCCTCTGAAAACCCTA GAGATAGGGCTTCTCCTTCGG	OP548103.1	*Bacillus cereus strain SPB-10*	100.00	1232	0.0
		OP546124.1	*Bacillus cereus strain OM3*	100.00	1232	0.0
		ON860698.1	*Bacillus cereus strain PSR21*	100.00	1232	0.0

5	AAAACGTGCCAGCAGCCGCGGTAATACGTAGGTGGCAAGCGTTGTCCGG AATTATTGGGCGTAAAGCGCGCGCAGGCGGTTTCTTAAGTCTGATGTGAA AGCCCCCGGCTCAACCGGGGAGGGTCATTGGAAACTGGGAAACTTGAGT GCAGAAGAGGAAAGTGGAATTCCAAGTGTAGCGGTGAAATGCGTAGAGA TTTGGAGGAACACCAGTGGCGAAGGCGACTTTCTGGTCTGTAACTGACGC TGAGGCGCGAAAGCGTGGGGAGCAAACAGGATTAGATACCCTGGTAGTC CACGCTGTAAACGATGAGTGCTAAGTGTTAGAGGGTTTCCGCCCTTTAGT GCTGAAGTTAACGCATTAAGCACTCCGCCTGGGGAGTACGGTCGCAAGAC TGAAACTCAAAGGAATTGACGGGGGCCCGCACAAGTGGTGGAGCATGTG GTTTAATTCGAAGCAACGCGAAGAACCTTACCAGGTCTTGACATCCTCTG ACAACCCTAGGGATAGGGCTTTCCCTTCGGGGACAGAGTGACAGGTGGT GCATGGTTGTCGTCAGCTCGTGTCGTGAGATGTTGGGTTAAGTCCCGCAA CGAGCGCAACCCTTGATCTTAGTTGCCAGCATTTAGTTGGGCACTCTAAG GTGACTGCCGGTGACAAACCGGAGGAAGGTGGGGATGACGTCAAATCAT CATGCCCCTTATGACCTGGGCTAC	MN543770.1	*Bacillus acidiceler strain CBD119*	100.00	1314	0.0
		MT378466.1	*Bacillus acidiceler strain J5R13LARS*	99.86	1314	0.0
		MT378465.1	*Bacillus acidiceler strain J5R12LARS*	99.86	1314	0.0
6	CCTTCCTCCGGTTTGTCACCGGCAGTCAACTTAGAGTGCCCAACTTAATG ATGGCAACTAAGCTTAAGGGTTGCGCTCGTTGCGGGACTTAACCCAACAT CTCACGACACGAGCTGACGACAACCATGCACCACCTGTCACTTTGTCCCC CGAAGGGGAAAGCTCTATCTCTAGAGTTGTCAAAGGATGTCAAGATTTGG TAAGGTTCTTCGCGTTGCTTCGAATTAAACCACATGCTCCACCGCTTGTGC GGGTCCCCGTCAATTCCTTTGAGTTTCAACCTTGCGGTCGTACTCCTCAGG CGGAGTGCTTAATGCGTTAGCTGCAGCACTAAGGGGCGGAAACCCCCTAA CACTTAGCACTCATCGTTTACGGCGTGGACTACCAGGGTATCTAATCCTGT TTGATCCCCACGCTTTCGCACATCAGCGTCAGTTACAGACCAGAAAGTCG CCTTCGCCACTGGTGTTCCTCCATATCTCTGCGCATTTCACCGCTACACATG GAATTCCACTTTCCTCTTCTGCACTCAAGTTTTCCAGTTTCCAATGACCCT CCACGGTTGAGCCGTGGGCTTTCACATCAGACTTAAAAAACCGCCTACGC GCGCTTTACGCCCAATAATTCCGGATAACGCTTGCCACCTACGTATTACCG CGGCTGCTGGCACGTAGTTAGCCGTGGCTTTCTGATTAGGTACCGTCAAG ACGTGCATAGTTACTTACACGTATGTTCTTCCCTAATAACAGAGTTTTACGA TCCGAAGACCTTCATCACTCACGCGGCGTTGCTCCGTCAGGCTTTCGCCC ATTGCGGAAGA	CP045187.2	*Staphylococcus haemolyticus strain VB19458*	99.88	1509	0.0
		MH930438.1	*Staphylococcus haemolyticus strain WY-8*	99.88	1509	0.0
		MN294491.1	*Staphylococcus haemolyticus strain RBRJ022*	99.88	1509	0.0
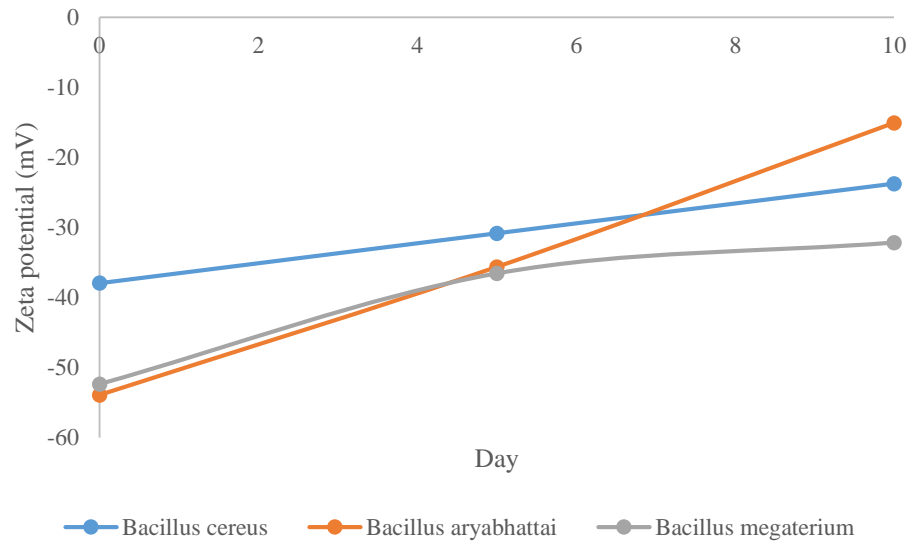
Figure above shows the value of zeta potential for *Bacillus aryabhattai, Bacillus megaterium* and *Bacillus cereus* respectively from day 0 to day 10. The results shows the zeta potential of all bacterial cells remained as negative value during 10-day bioleaching.

Standard deviation formula:

$$\sigma = \sqrt{(\Sigma(X - \text{mean})^2/(n - 1))}$$

where,

Σ = Sum

X = Sample data

N = Total number of sample data

Pooled standard deviation formula:

$$S_{\text{pooled}} = \sqrt{(((n_1-1)S_1^2 + (n_2-1)S_2^2 + \ldots + (n_k-1)S_k^2)/(n_1+n_2+\ldots+n_k-k))}$$

where,
n = Sample size
S = Standard deviation
k = Number of sample group

SEM images for raw kaolin:
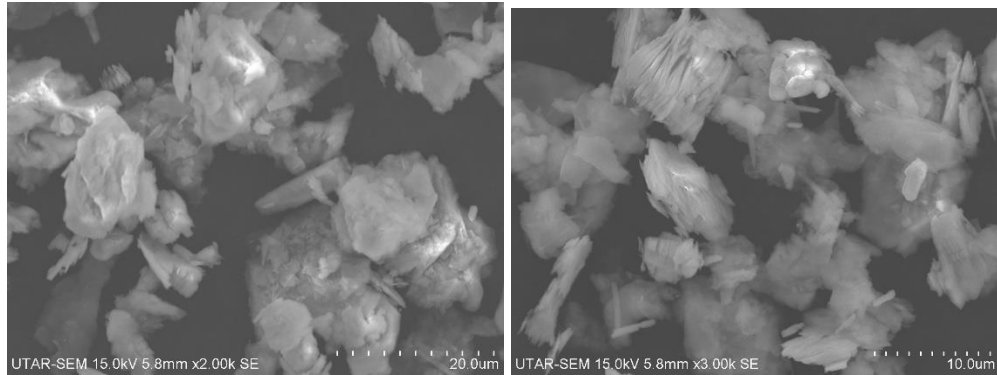
SEM images for abiotic control before bioleaching:
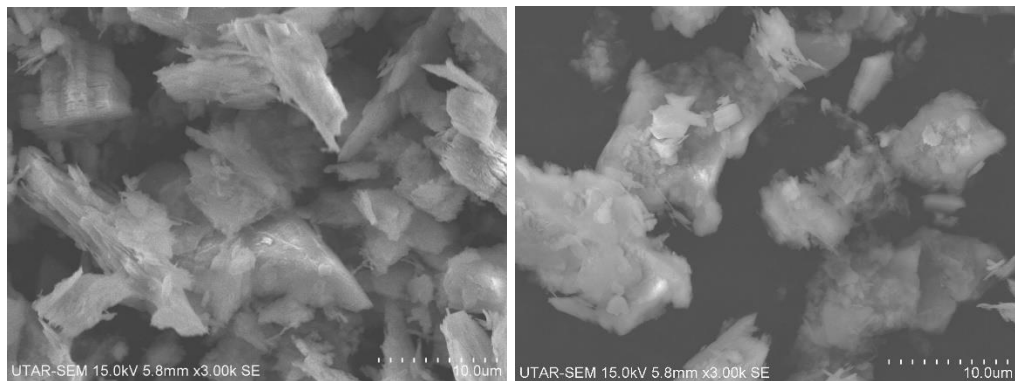
SEM images for abiotic control after bioleaching:
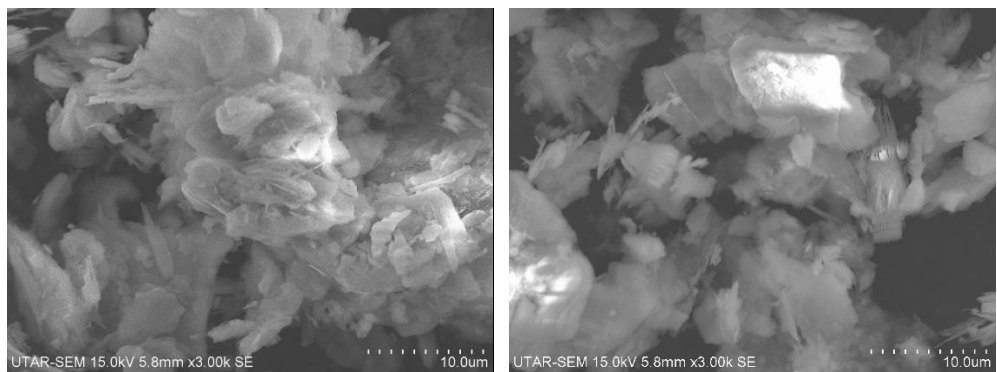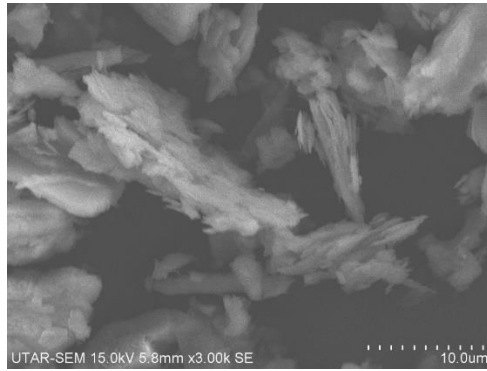
SEM images for sample with *B. cereus* before bioleaching:
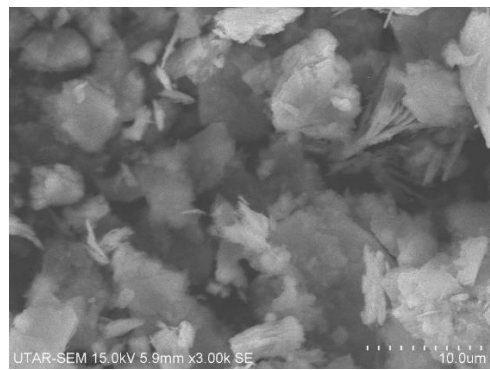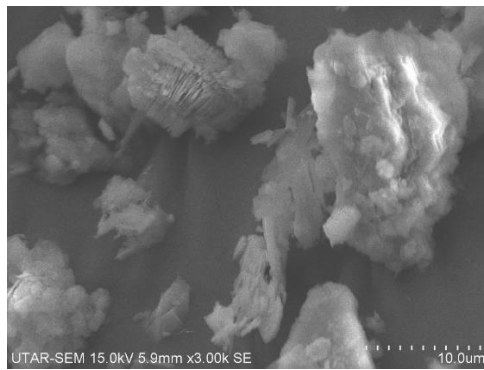
SEM images for sample with *B. cereus* after bioleaching:
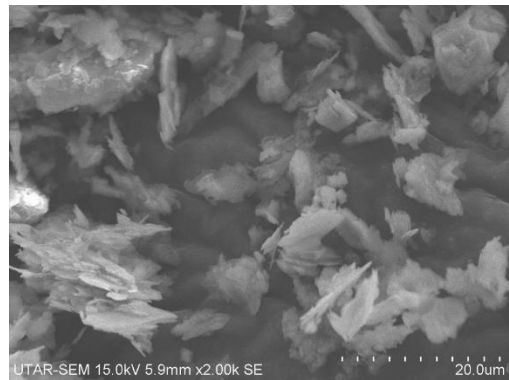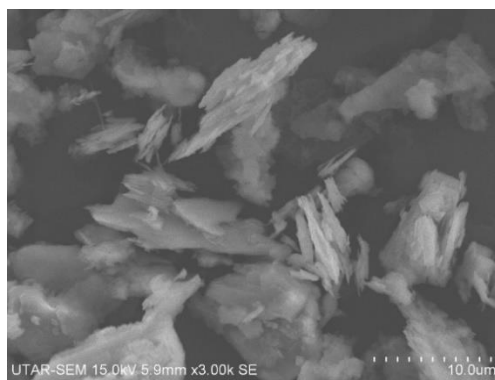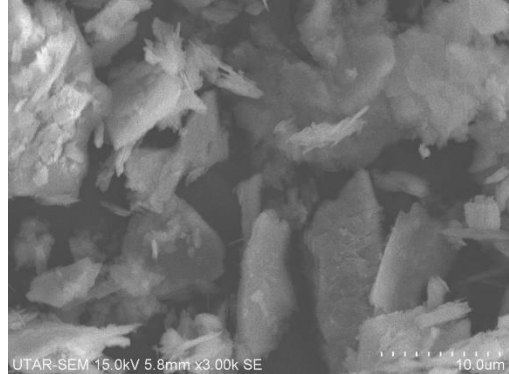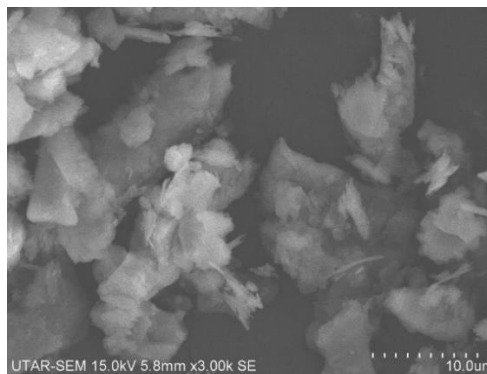

SEM images for sample with *B. aryabhattai* before bioleaching:
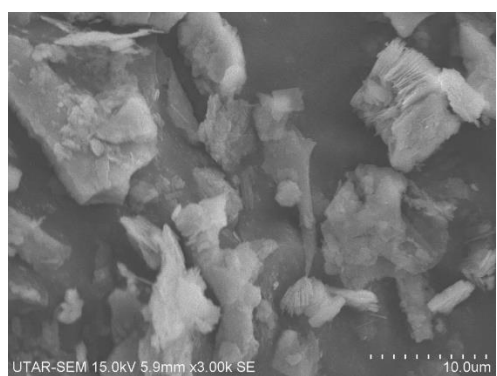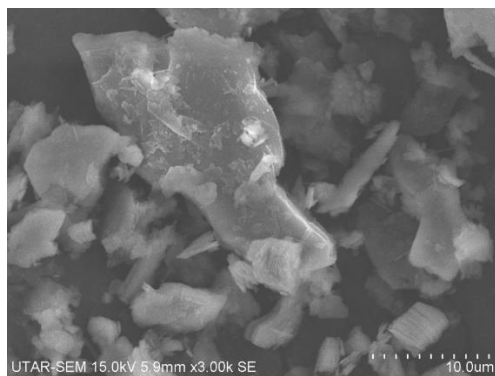
SEM images for sample with *B. aryabhattai* after bioleaching:
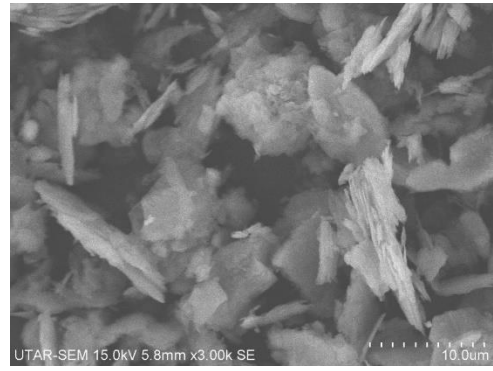
SEM images for sample with *B. megaterium* before bioleaching:

SEM images for sample with *B. megaterium* after bioleaching: